and that the extent of RIG-I 2CARD ubiquitination correlates strongly with its signal transduction activity.

Protein purification and mass spectrometry demonstrated that TRIM25 (also called oestrogen-responsive finger protein (EFP)[11]) is one of the proteins that associates with Flag–RIG-I(2CARD). TRIM25 has ubiquitin and ISG15 E3 ligase activity and downregulates 14-3-3σ through proteolysis for cell cycle regulation[12,13]. Co-immunoprecipitation revealed that RIG-I(2CARD) interacts with TRIM25 but not TRIM5-α, which has a similar structure to TRIM25 and functions as an intracellular inhibitor of retroviral replication[7] (Fig. 2a). Furthermore, interaction between Flag-tagged RIG-I or RIG-I(2CARD) and endogenous TRIM25 was readily detected in HEK293T cells (Fig. 2b). Confocal microscopy revealed that both RIG-I and TRIM25 exhibited punctate staining throughout the cytoplasm and that they co-localized extensively at cytoplasmic perinuclear bodies (Fig. 2c). As with other TRIM family members[7], TRIM25 contains a cluster of a RING-finger domain, a B box/coiled-coil domain (B Box/CCD) and a SPRY domain (Fig. 2d). Binding analysis revealed that the C-terminal SPRY domain of TRIM25 bound to both RIG-I and RIG-I(2CARD) as effectively as full-length TRIM25, whereas the RING-finger domain and B Box/CCD did not (Fig. 2d).

To test the role of TRIM25 in RIG-I ubiquitination, RIG-I or GST–RIG-I(2CARD) was co-expressed with wild-type TRIM25, E3 ligase-defective TRIM25(ΔRING) or TRIM5-α. TRIM25 expression markedly increased the ubiquitination levels of exogenous RIG-I and GST–RIG-I(2CARD), as well as endogenous RIG-I, but neither TRIM25(ΔRING) nor TRIM5-α had any effect (Fig. 3a, b; see also Supplementary Fig. 4a). In contrast, TRIM25 expression did not induce the ubiquitination of GST–MDA5(2CARD) (Supplementary Fig. 4b). TRIM25 depletion *in vivo* by a TRIM25-specific small hairpin RNA (shRNA)[13] significantly reduced the ubiquitination level of GST–RIG-I(2CARD) and RIG-I in a dose-dependent manner (Fig. 3c and Supplementary Fig. 5a), but a nonspecific scrambled-sequence shRNA had no effect on GST–RIG-I(2CARD) ubiquitination (Supplementary Fig. 5b). Finally, an *in vitro* ubiquitination assay showed that TRIM25 effectively delivered the ubiquitin moieties to maltose-binding protein (MBP)–T7-tagged RIG-I(2CARD), but not MBP–T7 alone or MBP–T7–RIG-I(2CARD(170stop)) (Fig. 3d and Supplementary Fig. 6a). Consistent with its ubiquitination level, RIG-I-mediated induction of IFN-β or NF-κB promoter activity considerably increased on TRIM25 expression in a dose-dependent manner (Fig. 3e and Supplementary Fig. 6b). Notably, expression of the TRIM25(SPRY) mutant, which was sufficient to bind to RIG-I, markedly suppressed GST–RIG-I(2CARD) ubiquitination in a dose-dependent manner (Fig. 3f) as well as endogenous RIG-I ubiquitination (Supplementary Fig. 4a). Furthermore, expression of the TRIM25(SPRY) mutant considerably decreased the RIG-I 2CARD-mediated activation of IFN-β or NF-κB promoter activity in a dose-dependent manner (Supplementary Fig. 7). This suggests that TRIM25-mediated ubiquitination has an important role in RIG-I signalling activity.

Unlike the GST–RIG-I(2CARD) K172R mutant, which showed an almost complete loss of ubiquitination and IFN-β and NF-κB promoter activation, GST–RIG-I(2CARD) K172only—containing five K→R substitutions but leaving K172 intact—demonstrated highly induced IFN-β and NF-κB promoter activity (Fig. 4a, b). Furthermore, the GST–RIG-I(2CARD) K172only mutant underwent robust ubiquitination (albeit lower than that of wild-type GST–RIG-I(2CARD)) on TRIM25 expression, whereas GST–RIG-I(2CARD) K172R was minimally ubiquitinated (Fig. 4c). However, despite a significant reduction in its level of ubiquitination, GST–RIG-I(2CARD) K172R interacted with TRIM25 as efficiently as wild-type GST–RIG-I(2CARD) and the K172only mutant (Fig. 4c). As seen with RIG-I(2CARD), full-length RIG-I K172only but not RIG-I K172R demonstrated ubiquitination at the same level as RIG-I wild type (Supplementary Fig. 8). Finally, correlated with their ubiquitination levels, expression of wild-type RIG-I and mutant RIG-I K172only in *RIG-I*$^{-/-}$ mouse embryonic fibroblasts (MEFs) induced IFN-β production on Sendai virus infection, whereas expression of mutant RIG-I K172R showed no effect on IFN-β production (Supplementary Fig. 9).

The 2CARD of RIG-I has been shown to bind to the MAVS CARD to elicit downstream signal transduction[14–17]. GST pull-down analysis showed that wild-type GST–RIG-I(2CARD) and mutant GST–RIG-I(2CARD) K172only efficiently interacted with the Flag-tagged CARD proline-rich domain of MAVS (Flag–MAVS(CARD-PRD)), whereas GST–RIG-I(2CARD) K172R and GST–RIG-I(2CARD) K99,169,172, 181,190,193R mutants poorly bound to Flag–MAVS(CARD-PRD) (Fig. 4d), indicating that Lys 172 is critical for TRIM25-mediated ubiquitination, RIG-I signalling and MAVS interaction, but not for TRIM25 binding (Fig. 4c).

Wild-type, *Trim25*$^{+/-}$ and *Trim25*$^{-/-}$ MEFs[18] were used to test the direct contribution of TRIM25 to RIG-I-mediated IFN-β expression. IFN-β promoter activity was very low in *Trim25*$^{-/-}$ MEFs and was reduced in *Trim25*$^{+/-}$ MEFs compared with wild-type MEFs

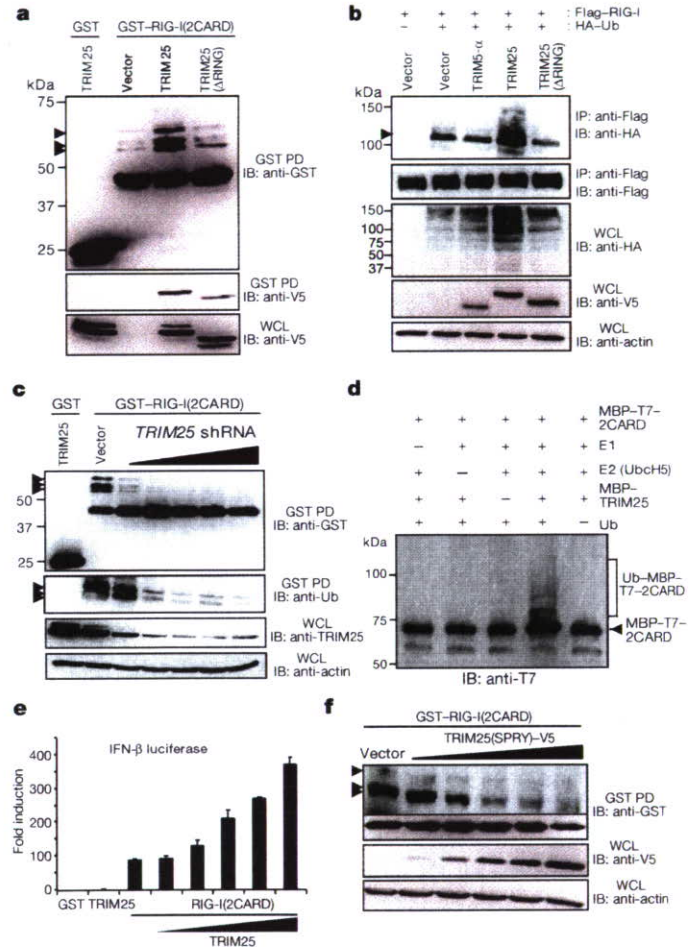

Figure 3 | TRIM25 is a primary E3 ubiquitin ligase of RIG-I. HEK293T cells transfected with GST or GST–RIG-I(2CARD) (**a**) or Flag–RIG-I and HA–ubiquitin (**b**) together with vector, TRIM25, TRIM25(ΔRING) or TRIM5-α were used for GST pull down (PD) (**a**) or immunoprecipitation with anti-Flag antibody (**b**). **c**, HEK293T cells transfected with GST or GST–RIG-I(2CARD) together with pSUPER.retro.puro or *TRIM25*-shRNA-specific pSUPER.retro.puro[13] were used for GST pull down. Arrows indicate the ubiquitinated GST–RIG-I(2CARD) and Flag–RIG-I. **d**, *In vitro* ubiquitination was detected by anti-T7 immunoblotting. **e**, IFN-β luciferase activity in HEK293T cells transfected with GST–RIG-I(2CARD) and TRIM25. The results are expressed as means ± s.d. ($n = 3$). **f**, HEK293T cells transfected with GST–RIG-I(2CARD) and V5–TRIM25(SPRY) were used for GST pull down. Arrows indicate ubiquitinated GST–RIG-I(2CARD).

(Supplementary Fig. 10a). Consistent with IFN-β promoter activation, virus-induced IFN-β production was virtually undetectable in *Trim25*$^{-/-}$ MEFs, whereas it was considerably high in wild-type MEFs (Fig. 4e). *Trim25*$^{+/-}$ MEFs showed a slightly reduced level of IFN-β production compared with wild-type MEFs (Fig. 4e). On vesicular stomatitis virus (VSV)–enhanced green fluorescent protein (eGFP) infection at various multiplicity of infections (MOIs), *Trim25*$^{-/-}$ MEFs showed remarkably increased levels of VSV–eGFP-positive cells (Fig. 4g and Supplementary Fig. 10b) and increased VSV yields (over 100-fold) (Fig. 4f) compared with wild-type and *Trim25*$^{+/-}$ MEFs. Similarly, *Trim25*$^{-/-}$ MEFs showed a considerable increase in the level of Newcastle disease virus (NDV)–GFP infection (Supplementary Fig. 10c). Finally, TRIM25 expression significantly suppressed VSV–eGFP replication in HEK293T cells, whereas expression of the TRIM25(SPRY) mutant detectably increased VSV–eGFP replication (Fig. 4h). Collectively, these results indicate that TRIM25 is critical for cytosolic RIG-I signal transduction that mediates the induction of the IFN response on viral infection.

Ubiquitination is a versatile post-translational modification involved in various cellular functions[19]. Our study indicates that TRIM25 E3 ubiquitin ligase induces the Lys 63-linked ubiquitination of RIG-I; that Lys 172 is the critical site for TRIM25-mediated ubiquitination; and that, as seen with the ubiquitin-dependent interaction between RIP and NEMO[20], the TRIM25-mediated ubiquitination of RIG-I may facilitate its interaction with MAVS, which ultimately leads to downstream signal transduction. Thus, the interconnection between the RIG-I cytosolic viral RNA receptor and a member of the TRIM family represents a new class of antiviral regulatory pathway involved in innate immunity.

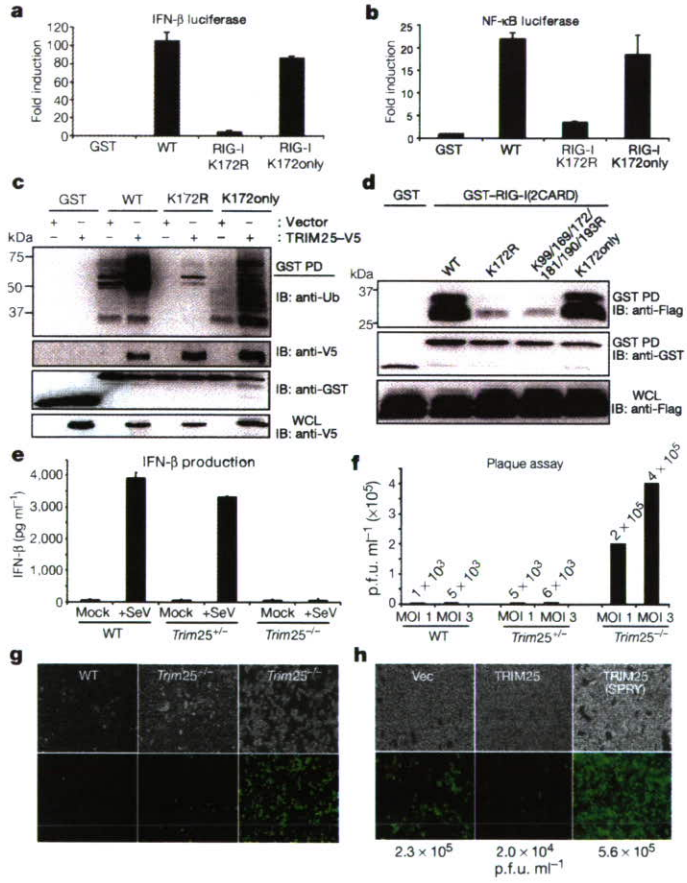

Figure 4 | Role of TRIM25-mediated ubiquitination in RIG-I antiviral activity. IFN-β (**a**) and NF-κB (**b**) promoter activity in GST–RIG-I(2CARD) or mutant transfected cells. The results are expressed as means ± s.d. ($n = 3$). **c**, HEK293T cells transfected with GST–RIG-I(2CARD), GST–RIG-I(2CARD) K172R, or GST–RIG-I(2CARD) K172only together with vector or TRIM25 were used for GST pull down. **d**, HEK293T cells transfected with GST–RIG-I(2CARD) or the indicated mutants together with Flag–MAVS(CARD-PRD) were used for GST pull down. **e**, IFN-β production in wild-type, *Trim25*$^{+/-}$ and *Trim25*$^{-/-}$ MEFs upon Sendai virus infection. The results are expressed as means ± s.d. ($n = 3$). **f–h**, VSV–eGFP replication in wild-type, *Trim25*$^{+/-}$ and *Trim25*$^{-/-}$ MEFs (**f** and **g**) or in vector-, TRIM25-, or TRIM25(SPRY)-expressing HEK293T cells (**h**) was determined by plaque assay or visualized by fluorescence microscopy.

METHODS SUMMARY

RNA interference for TRIM25. The mammalian expression vector pSUPER.retro.puro (OligoEngine), encoding shRNAs for *TRIM25* sequence, was provided by D.-E. Zhang. Details of the shRNA sequence and transfection method have been described[13].

Viruses. NDV–GFP and VSV–eGFP were provided by A. Garcia-Sastre and S. Whelan, respectively.

Measurement of IFN-β production. Cell culture supernatants were collected and analysed for IFN-β production using enzyme-linked immunosorbent assays (PBL Biomedical Laboratories).

***In vitro* ubiquitination assay.** Purified MBP–T7–RIG-I(2CARD) (20 μg ml^{-1}) and MBP–TRIM25 (20 μg ml^{-1}) derived from *Escherichia coli* were incubated in a reaction buffer (50 mM Tris-HCl, 2 mM dithiothreitol, 5 mM $MgCl_2$ and 4 mM ATP) with ubiquitin (50 μg ml^{-1}; Sigma), human recombinant E1 (1.6 μg ml^{-1}; BIOMOL) and human recombinant UbcH5a (20 μg ml^{-1}; BIOMOL) at 32 °C for 2 h and subjected to immunoblotting with anti-T7 antibody (Novagen).

Full Methods and any associated references are available in the online version of the paper at www.nature.com/nature.

Received 14 February; accepted 8 March 2007.
Published online 28 March 2007.

1. Honda, K., Takaoka, A. & Taniguchi, T. Type I interferon gene induction by the interferon regulatory factor family of transcription factors. *Immunity* 25, 349–360 (2006); erratum 25, 849 (2006).
2. Hornung, V. *et al.* 5′-Triphosphate RNA is the ligand for RIG-I. *Science* **314**, 994–997 (2006).
3. Meylan, E. & Tschopp, J. Toll-like receptors and RNA helicases: two parallel ways to trigger antiviral responses. *Mol. Cell* **22**, 561–569 (2006).
4. Pichlmair, A. *et al.* RIG-I-mediated antiviral responses to single-stranded RNA bearing 5′-phosphates. *Science* **314**, 997–1001 (2006).
5. Stetson, D. B. & Medzhitov, R. Antiviral defense: interferons and beyond. *J. Exp. Med.* **203**, 1837–1841 (2006).
6. Yoneyama, M. *et al.* The RNA helicase RIG-I has an essential function in double-stranded RNA-induced innate antiviral responses. *Nature Immunol.* **5**, 730–737 (2004).
7. Nisole, S., Stoye, J. P. & Saib, A. TRIM family proteins: retroviral restriction and antiviral defence. *Nature Rev. Microbiol.* **3**, 799–808 (2005).
8. Johnson, C. L. & Gale, M. Jr. CARD games between virus and host get a new player. *Trends Immunol.* **27**, 1–4 (2006).
9. Meylan, E., Tschopp, J. & Karin, M. Intracellular pattern recognition receptors in the host response. *Nature* **442**, 39–44 (2006).
10. Kato, H. *et al.* Cell type-specific involvement of RIG-I in antiviral response. *Immunity* **23**, 19–28 (2005).
11. Orimo, A., Inoue, S., Ikeda, K., Noji, S. & Muramatsu, M. Molecular cloning, structure, and expression of mouse estrogen-responsive finger protein Efp. Co-localization with estrogen receptor mRNA in target organs. *J. Biol. Chem.* **270**, 24406–24413 (1995).
12. Urano, T. *et al.* Efp targets 14-3-3σ for proteolysis and promotes breast tumour growth. *Nature* **417**, 871–875 (2002).
13. Zou, W. & Zhang, D. E. The interferon-inducible ubiquitin-protein isopeptide ligase (E3) EFP also functions as an ISG15 E3 ligase. *J. Biol. Chem.* **281**, 3989–3994 (2006).
14. Meylan, E. *et al.* Cardif is an adaptor protein in the RIG-I antiviral pathway and is targeted by hepatitis C virus. *Nature* **437**, 1167–1172 (2005).
15. Seth, R. B., Sun, L., Ea, C. K. & Chen, Z. J. Identification and characterization of MAVS, a mitochondrial antiviral signaling protein that activates NF-κB and IRF 3. *Cell* **122**, 669–682 (2005).
16. Xu, L. G. *et al.* VISA is an adapter protein required for virus-triggered IFN-β signaling. *Mol. Cell* **19**, 727–740 (2005).
17. Kawai, T. *et al.* IPS-1, an adaptor triggering RIG-I- and Mda5-mediated type I interferon induction. *Nature Immunol.* **6**, 981–988 (2005).
18. Orimo, A. *et al.* Underdeveloped uterus and reduced estrogen responsiveness in mice with disruption of the estrogen-responsive finger protein gene, which is a direct target of estrogen receptor α. *Proc. Natl Acad. Sci. USA* **96**, 12027–12032 (1999).

19. Haglund, K. & Dikic, I. Ubiquitylation and cell signaling. *EMBO J.* **24**, 3353–3359 (2005).
20. Ea, C. K., Deng, L., Xia, Z. P., Pineda, G. & Chen, Z. J. Activation of IKK by TNFα requires site-specific ubiquitination of RIP1 and polyubiquitin binding by NEMO. *Mol. Cell* **22**, 245–257 (2006).
21. Kirkpatrick, D. S., Denison, C. & Gygi, S. P. Weighing in on ubiquitin: the expanding role of mass-spectrometry-based proteomics. *Nature Cell Biol.* **7**, 750–757 (2005).

Supplementary Information is linked to the online version of the paper at www.nature.com/nature.

Acknowledgements This work was supported by US Public Health Service grants (J.U.J.), the exchange programme between Harvard Medical School and the graduate training programme 1071 at the Friedrich-Alexander University Erlangen-Nuremberg, Germany (M.U.G.), and a Korea Research Foundation Grant (C.-H.J.). We thank A. Garcia-Sastre, D.-E. Zhang and S. Whelan for providing reagents, and R. Tomaino and J. Nagel for mass spectrometry. We also thank all members of the Tumor Virology Division, New England Primate Research Center, for discussions.

Author Contributions M.U.G. performed all aspects of this study. Y.C.S., C.-H.J. and C.L. assisted in experimental design and in collecting the data. T.U. and S.I. performed the *in vitro* ubiquitination assay and generated *Trim25*$^{-/-}$ MEFs. L.S. and Z.C. generated the MAVS construct and RIG-I antibody. T.O. and S.A. generated the RIG-I construct and *RIG-I*$^{-/-}$ MEFs. M.U.G. and J.U.J. organized this study and wrote the paper. All authors discussed the results and commented on the manuscript.

Author Information Reprints and permissions information is available at www.nature.com/reprints. The authors declare no competing financial interests. Correspondence and requests for materials should be addressed to J.U.J. (jae_jung@hms.harvard.edu).

METHODS

Cell culture. HEK293T, MEF and Hela cells were cultured in Dulbecco's modified Eagle's medium supplemented with 10% fetal bovine serum, 2 mM L-glutamine and 1% penicillin-streptomycin (Gibco-BRL). Transient transfections were performed with FuGENE 6 (Roche), lipofectamine 2000 (Invitrogen), or calcium phosphate (Clontech) following the manufacturer's instructions. Wild-type, *Trim25*$^{+/-}$ and *Trim25*$^{-/-}$ MEFs were immortalized with LXSN-E6/E7 retroviral vector containing human papilloma virus 16 E6 and E7 oncogenes using a standard protocol of selection with 200 μg ml^{-1} of neomycin. *RIG-I*$^{-/-}$ MEFs were infected with pBabe-puro vector, pBabe-puro-RIG-I wild-type, pBabe-puro-RIG-I K172R, or pBabe-puro-RIG-I K172only retrovirus, followed by selection with 1 μg ml^{-1} of puromycin.

Plasmid construction. All constructs for transient and stable expression in mammalian cells were derived from the pEBG GST fusion vector and the pEF-IRES-Puro expression vector. DNA fragments corresponding to the coding sequence of the *RIG-I* and *TRIM25* genes were amplified from template DNA by polymerase chain reaction (PCR) and subcloned into plasmid pEBG between restriction sites *Kpn*I and *Not*I or pEF-IRES-puro between *Afl*II and *Not*I for selection of stable transfectants. V5-tagged TRIM25 and Flag-tagged RIG-I were expressed from a modified pIRES-puro encoding a C-terminal V5 tag and Flag tag, respectively. RIG-I mutants were generated by PCR using site-directed mutagenesis. All constructs were sequenced using an ABI PRISM 377 automatic DNA sequencer to verify 100% agreement with the original sequence.

***In vivo* GST pull down, protein purification and mass spectrometry.** At 48 h after transfection with vectors expressing GST, GST–RIG-I(2CARD) or GST–MDA5(2CARD) fusions, HEK293T cells were collected and lysed with NP40 buffer (50 mM HEPES, pH 7.4, 150 mM NaCl, 1 mM EDTA, 1% (v/v) NP40) supplemented with a complete protease inhibitor cocktail (Roche). Post-centrifuged supernatants were pre-cleared with protein A/G beads at 4 °C for 2 h. Pre-cleared lysates were mixed with a 50% slurry of glutathione-conjugated Sepharose beads (Amersham Biosciences), and the binding reaction was incubated for 4 h at 4 °C. Precipitates were washed extensively with lysis buffer. Proteins bound to glutathione beads were eluted and separated on a NuPAGE 4–12% Bis-Tris gradient gel (Invitrogen). After Coomassie or silver staining (Invitrogen), specific protein bands were excised and analysed by ion-trap mass spectrometry at the Harvard Taplin Biological Mass Spectrometry facility, and amino acid sequences were determined by tandem mass spectrometry and database searches.

Immunoblot analysis and immunoprecipitation assay. For immunoblotting, polypeptides were resolved by SDS–polyacrylamide gel electrophoresis (SDS–PAGE) and transferred to a PVDF membrane (Bio-Rad). Immunodetection was achieved with anti-V5 (1:5,000) (Invitrogen), anti-Flag (1:5,000) (Sigma), anti-HA (1:5,000), anti-GST (1:10,000) (Sigma), anti-actin (1:10,000) (Abcam), or anti-TRIM25 (1:2,000) (BD Bioscience) antibodies. The proteins were visualized by a chemiluminescence reagent (Pierce) and detected by a Fuji Phosphor Imager.

For immunoprecipitation, cells were collected after 48 h and then lysed in NP40 buffer supplemented with a complete protease inhibitor cocktail (Roche). After pre-clearing with protein A/G agarose beads for 2 h at 4 °C, whole-cell lysates were used for immunoprecipitation with the indicated antibodies. Generally, 1–2 μg of commercial antibody was added to 1 ml of cell lysate, which was incubated at 4 °C for 4–12 h. After addition of protein A/G agarose beads, the incubation was continued for 2 h. Immunoprecipitates were extensively washed with lysis buffer and eluted with SDS loading buffer by boiling for 5 min.

Confocal immunofluorescence microscopy. Eighteen to twenty-four hours after transfection, cells were fixed with 4% paraformaldehyde for 15 min, permeabilized with 0.2% (v/v) Triton X-100 for 15 min, blocked with 10% goat serum in PBS for 1 h and reacted with diluted primary antibody in 1% goat serum for up to 2 h at room temperature. After incubation, cells were washed extensively with PBS, incubated with the appropriate secondary antibody diluted in 1% goat serum for 1 h at room temperature, and washed three times with PBS. Confocal microscopy was performed using a Leica TCS SP laser-scanning microscope (Leica Microsystems) fitted with a ×100 Leica objective (PL APO, 1.4NA) and Leica imaging software. Images were collected at 512 × 512-pixel resolution. The stained cells were optically sectioned in the *z* axis, and the images in the different channels (photo multiplier tubes) were collected simultaneously. The step size in the *z* axis varied from 0.2 to 0.5 μm to obtain 16 slices per imaged file. The images were transferred to a Macintosh G4 computer (Apple Computer), and Photoshop (Adobe) was used to render the images.

Vitamin K_2 induces phosphorylation of protein kinase A and expression of novel target genes in osteoblastic cells

T Ichikawa[1], K Horie-Inoue[1], K Ikeda[1], B Blumberg[2] and S Inoue[1,3]

[1]Division of Gene Regulation and Signal Transduction, Research Center for Genomic Medicine, Saitama Medical University, Hidaka-shi, Saitama 350-1241, Japan

[2]Department of Developmental and Cell Biology, University of California, Irvine, California 92697-2300, USA

[3]Department of Geriatric Medicine, Graduate School of Medicine, The University of Tokyo, 7-3-1 Hongo, Bunkyo-ku, Tokyo 113-8655, Japan

(Correspondence should be addressed to S Inoue; Email: inoue-ger@h.u-tokyo.ac.jp)

Abstract

Vitamin K is known as a critical nutrient required for bone homeostasis and blood coagulation, and it is clinically used as a therapeutic agent for osteoporosis in Japan. Besides its enzymatic action as a cofactor of vitamin K-dependent γ-glutamyl carboxylase (GGCX), we have previously shown that vitamin K_2 is a transcriptional regulator of bone marker genes and extracellular matrix-related genes, by activating the steroid and xenobiotic receptor (SXR). To explore a novel action of vitamin K in osteoblastic cells, we identified genes up-regulated by a vitamin K_2 isoform menaquinone-4 (MK-4) using oligonucleotide microarray analysis. Among these up-regulated genes by MK-4, growth differentiation factor 15 (GDF15) and stanniocalcin 2 (STC2) were identified as novel *MK-4* target genes independent of GGCX and SXR pathways in human and mouse osteoblastic cells. The induction of GDF15 and STC2 is likely specific to MK-4, as it was not exerted by another vitamin K_2 isoform MK-7, vitamin K_1, or the MK-4 side chain structure geranylgeraniol. Investigation of the involved signaling pathways revealed that MK-4 enhanced the phosphorylation of protein kinase A (PKA), and the MK-4-dependent induction of both *GDF15* and *STC2* genes was reduced by the treatment with a PKA inhibitor H89 or siRNA against PKA. These results suggest that vitamin K_2 modulates its target gene expression in osteoblastic cells through the PKA-dependent mechanism, which may be distinct from the previously known vitamin K signaling pathways.

Journal of Molecular Endocrinology (2007) **39,** 239–247

Introduction

Vitamin Ks are fat-soluble 2-methyl-1,4-naphthoquinone-related compounds, including natural phylloquinone (K_1) and menaquinones (K_2). Vitamins K_1 and K_2 differ only in the substituent group. Vitamin K_1 possesses a phytyl group (partially saturated polyisoprenoid group), whereas K_2 possesses a repeating, unsaturated *trans*-polyisoprenyl group. Menaquinones include a range of related forms generally designated as menaquinone-*n* (MK-*n*), where *n* is the number of isoprenyl groups. Vitamin Ks play a role in the bone-building process as well as classic blood coagulation pathway. Indeed, clinical studies have demonstrated that vitamin K_2 is an effective treatment for osteoporosis and preventing fractures (Booth *et al.* 2000, Shiraki *et al.* 2000). Menaquinone-4 (MK-4), one of the vitamin K_2 containing four isoprene units, is frequently prescribed for osteoporosis in Japan.

One of the notable molecular functions of vitamin K is as a cofactor for vitamin K-dependent γ-glutamyl carboxylase (GGCX). GGCX catalyzes the post-translational modification of specific glutamates to γ-carboxyglutamate (Gla) in a number of proteins. Most vitamin K-dependent proteins are involved in the hemostatic process and are associated with bone metabolism. Osteocalcin (bone Gla protein), and matrix Gla protein (MGP) are two major Gla proteins in bone and γ-carboxylated proteins are important in bone metabolism. Osteocalcin serves as a good biochemical marker of the metabolic turnover of bone because osteocalcin lacking Gla residues cannot bind to hydroxyapatite, one of the major components of bone matrix (Nishimoto & Price 1985, Vergnaud *et al.* 1997). Moreover, levels of undercarboxylated osteocalcin increase during aging and significantly correlate with fracture risk (Vergnaud *et al.* 1997).

MGP is predominantly expressed and produced in chondrocytes and vascular smooth muscle cells (Luo *et al.* 1997, Shanahan & Weissberg 1998). Data from rodent studies revealed that MGP plays a key role in the inhibition of tissue calcification. Luo *et al.* (1997) reported that MGP-deficient mice showed excessive cartilage formation and growth plate mineralization, resulting in impaired growth of the long bones. Thus, vitamin K plays a significant role in bone homeostasis through γ-carboxylated proteins. On the other hand, we previously reported that vitamin K_2 has a

Journal of Molecular Endocrinology (2007) **39,** 239–247
0952–5041/07/039–239

DOI: 10.1677/JME-07-0048
Online version via http://www.endocrinology-journals.org

transcriptional regulatory function in addition to its role as an enzyme cofactor (Tabb *et al.* 2003). Vitamin K_2 was a ligand of the steroid and xenobiotic receptor (SXR), and both vitamin K_2 and the known SXR ligands rifampicin (RIF) up-regulated expression of the prototypical *SXR* target gene cytochrome P450 (CYP) 3A4 and bone marker genes, such as alkaline phosphatase and osteoprotegerin (Tabb *et al.* 2003). Furthermore, we identified SXR-dependent vitamin K_2 target genes that participated in extracellular matrix formation in osteoblastic cells (Ichikawa *et al.* 2006). These findings suggested an important role for vitamin K_2-dependent transcriptional regulation in bone homeostasis. Meanwhile, during our microarray analyses that identify the *SXR* target genes using osteoblastic cells treated with RIF or vitamin K_2, we found that a number of genes were specifically up-regulated by vitamin K_2 but not RIF. This observation suggested that potentially novel mechanism could be associated with the up-regulation of these genes by vitamin K_2.

In the present study, we screened for genes induced by MK-4 in osteoblastic MG63 cells using microarray analysis, and identified several vitamin K_2-target genes. Here, we focused on the growth differentiation factor 15 (GDF15) and stanniocalcin 2 (*STC2*) genes as MK-4 targets. We found that other vitamin Ks, geranylgeraniol (GGO), and SXR agonists failed to induce the expression of *GDF15* and *STC2* genes, although a protein kinase A (PKA) activator forskolin (FSK) induced the expression of both genes. Our findings indicate that GDF15 and STC2 are regulated by a PKA-dependent, GGCX- and SXR-independent pathways.

Materials and methods

Materials

RIF was purchased from Nacalai Tesque (Kyoto, Japan). Vitamin K_1, GGO, and FSK were purchased from Sigma. MK-4 and MK-7 were gifts of Eisai Co. Ltd (Tokyo, Japan). H89 was obtained from BioMol (Plymouth Meeting, PA, USA).

Cell culture and generation of stable cell lines expressing SXR

MG63 human osteosarcoma cells were grown in Dulbecco's modified Eagle's medium supplemented with 10% fetal bovine serum (FBS), 50 U/ml penicillin, and 50 μg/ml streptomycin. Mouse MC3T3-E1 osteoblastic cells were maintained in α-minimum essential medium (MEM) supplemented with 10% FBS, 50 U/ml penicillin, and 50 μg/ml streptomycin. Prior to vitamin K treatment, cells were cultured in phenol red-free

Table 1 Common up-regulated genes by 48-h treatment with menaquinone-4 (MK-4; 10 μM) in both MG63/vector and MG63/Flag-VP16C-SXR stable cell lines identified by GeneChip analysis

				Fold change	
	Ensemble gene ID	**Gene symbol**	**Description**	MG63/vector	MG63/Flag-VP16C-SXR
Probe set ID					
221577_x_at	ENSG00000130513	*GDF15*	Growth differentiation factor 15	8·00	5·66
218145_at	ENSG00000101255	*TRIB3*	Tribbles homolog 3 (*Drosophila*)	6·50	4·29
207145_at	ENSG00000138379	*GDF8*	Growth differentiation factor 8	4·29	2·00
219270_at	ENSG00000128965	*MGC4504*	Hypothetical protein MGC4504	3·03	3·48
202847_at	ENSG00000100889	*PCK2*	Phosphoenolpyruvate carboxykinase 2 (mitochondrial)	2·46	2·00
205047_s_at	ENSG00000070669	*ASNS*	Asparagine synthetase	2·46	3·25
203665_at	ENSG00000100292	*HMOX1*	Heme oxygenase (decycling) 1	2·30	2·46
206026_s_at	ENSG00000123610	*TNFAIP6*	Tumor necrosis factor, α-induced protein 6	2·30	2·00
203438_at	ENSG00000113739	*STC2*	Stanniocalcin 2	2·14	2·00
203477_at	ENSG00000204291	*COL15A1*	Collagen, type XV, α 1	2·14	2·14
206025_s_at	ENSG00000123610	*TNFAIP6*	Tumor necrosis factor, α-induced protein 6	2·14	2·46
209921_at	ENSG00000151012	*SLC7A11*	Solute carrier family 7, member 11	2·14	2·64
202887_s_at	ENSG00000168209	*DDIT4*	DNA-damage-inducible transcript 4	2·00	2·64
204422_s_at	ENSG00000138685	*FGF2*	Fibroblast growth factor 2 (basic)	2·00	2·30
220892_s_at	ENSG00000135069	*PSAT1*	Phosphoserine aminotransferase 1	2·00	2·00

MG63/vector and MG63/Flag-VP16C-SXR cells are stably expressing Flag-pcDNA3 vector and pcDNA3-Flag-VP16C-SXR respectively. Twofold or more up-regulated genes by MK-4 over vehicle in both cells were selected, except SXR-dependent up-regulated ones with the ratios of fold change in MG63/Flag-VP16C-SXR versus MG63/vector by ≥1·5-fold. Gene annotation was determined based on the probe set ID by the Array Finder on the Affymetrix web site (http://www.affymetrix.com).

media containing 10% dextran–charcoal stripped FBS (dcc-FBS). N-terminally Flag-tagged pcDNA3 (Invitrogen) plasmids containing VP16C-SXR (pcDNA3-Flag-VP16C-SXR) were previously described (Ichikawa *et al.* 2006). VP16C-SXR contained 20 amino acids from the C-terminus of VP16 activation domain upstream of SXR. Generation of MG63 cell lines stably expressing pcDNA3-Flag-VP16C-SXR (MG63/Flag-VP16C-SXR) or the empty vector Flag-tagged pcDNA3 (MG63/vector) were previously described (Ichikawa *et al.* 2006).

Western blot analysis

Whole cell lysates were prepared using a lysis buffer (50 mM HEPES (pH 7·5), 150 mM NaCl, 10% glycerol, 1% Triton X-100, 1·5 mM $MgCl_2$, 1 mM sodium orthovanadate, 10 μg/ml aprotinin, and 10 μg/ml leupeptin). Protein concentrations were analyzed using the BCA protein assay kit (Pierce Biotechnology, Rockford, IL, USA). Proteins were resolved by SDS-PAGE and electroblotted onto Immobilon-P Transfer Membrane (Millipore, Billerica, MA, USA). The antibody–antigen complexes were detected using the Western Blotting Chemiluminescence Luminol Reagent (Santa Cruz Biotechnology, Santa Cruz, CA, USA). Antibodies used included anti-phospho PKA and anti-PKA (Cell Signaling Technology, Danvers, MA, USA).

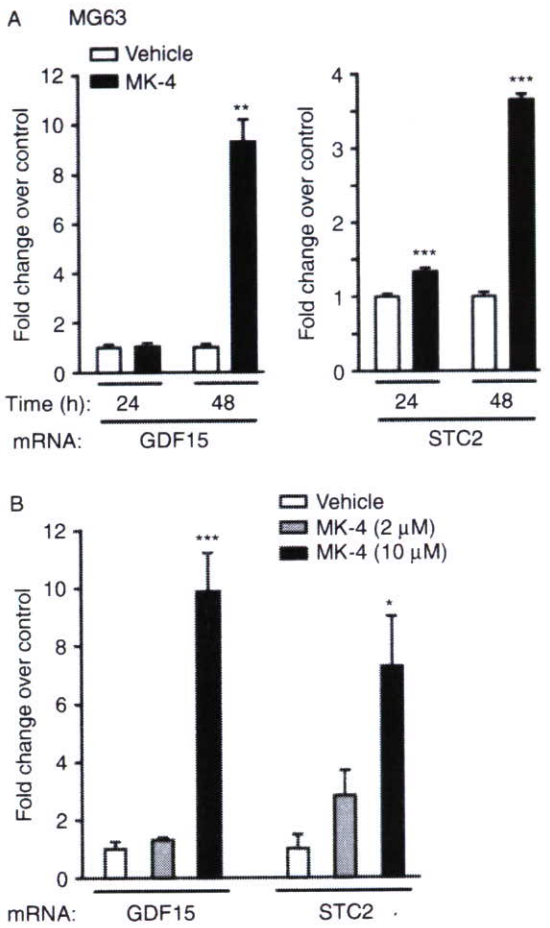

Figure 1 Up-regulation of growth differentiation factor 15 (GDF15) and stanniocalcin-2 (STC2) mRNA levels by a vitamin K_2 isoform menaquinone-4 (MK-4) in osteoblastic cells. Human osteoblastic MG63 cells were treated with MK-4 (10 μM) or vehicle for the indicated times (A), and mouse osteoblastic MC3T3-E1 cells were treated with MK-4 (2 or 10 μM) or vehicle for 48 h (B). mRNA levels for GDF15 and STC2 were determined by quantitative RT-PCR (qRT-PCR). Data are representative of experiments with similar results, each performed in triplicate. $^*P<0{\cdot}05$, $^{**}P<0{\cdot}01$, $^{***}P<0{\cdot}001$ when compared with control cells treated with vehicle.

Preparation of cRNA and oligonucleotide array hybridization

Total RNA was extracted from MG63/vector and MG63/Flag-VP16C-SXR cells treated with vehicle (0·1% ethanol) and MK-4 (10 μM) for 48 h. The methods for preparation of cRNA and subsequent steps leading to hybridization and scanning of the U133A GeneChip Arrays Station (Affymetrix, Santa Clara, CA, USA) were performed as described previously (Ichikawa *et al.* 2006). Data analysis was performed using Affymetrix Microarray Suite software. For comparing arrays, normalization was performed using data from all probe sets.

Quantitative reverse transcription PCR analysis

Osteoblastic cells were treated with RIF, MK-4, MK-7, vitamin K_1, GGO, FSK, or vehicle for indicated times. Total RNA was isolated using the ISOGEN reagent (Nippon gene, Tokyo, Japan). First, strand cDNA was generated from RNase-free DNase I-treated total RNA using the SuperScript II Reverse Transcriptase (Invitrogen) and oligo-dT_{20} primer. For PCR amplification, the primer sequences were: human GDF15, 5′-GAAACGCTACGAGGACCTGCTA-3′ and 5′-ACGAGGTCGGTGTTCGAATC-3′; human STC2, 5′-TGGGATTTGCATGACTTTTCTG-3′ and 5′-GGCGTCTTTGATGAATGACTTG-3′; human GGCX, 5′-CTTGAGACCCTTTGAGGCAGTT-3′ and 5′-GGATTTGACTCAGGAGGATTAGAATG-3′; human CYP3A4, 5′-TTCAGCCCATCTCCTTTCATATTT-3′ and 5′-CAGTTGGGTGTTGAGGATGGA-3′; human α-catalytic subunit of PKA (PRKACA), 5′-CAACTTTCCGTTCCTCGTCAA-3′ and 5′-CGCCGGGCACGTACTC-3′; human glyceraldehyde-3-phosphate dehydrogenase (GAPDH), 5′-GCCTGCCTGACCAAATGC-3′ and 5′-GTGGTCGTTGAGGGCAATG-3′; mouse GDF15, 5′-AGACTGTGCAGGCAACTCTTGA-3′ and 5′-ACACTCGCCCACGCACAT-3′; mouse STC2, 5′-CAACTCTTGTGAAATCCAGGGTTT-3′ and 5′-CATCGAATTTTCCAGCGTTGT-3′; and mouse GAPDH, 5′-GCATGGCCTTCCGTGTTC-3′ and 5′-TGTCATCAT-

132# ACTTGGCAGGTTTCT-3′. mRNAs were quantified by real-time PCR using SYBR green PCR master mix (Applied Biosystems, Foster City, CA, USA) and the ABI Prism 7000 system (Applied Biosystems) as previously described (Ichikawa *et al.* 2006).

RNA interference

Small interfering RNA (siRNA) duplexes to target human GGCX (D-009856-02) and PRKACA (D-004649-01) were purchased from Dharmacon Research Inc. (Lafayette, CO, USA). An siRNA specific to luciferase gene (Luciferase GL2 Duplex, Dharmacon) was used as a control. Cells were transfected with siRNA using GeneSilencer reagent (Genlantis, San Diego, CA, USA) for indicated times in the culture medium containing 10% dcc-FBS in the presence or absence of MK-4.

Statistical analysis

Differences between two groups were analyzed using two-sample, two-tailed Student's *t*-test. A P value $<0{\cdot}05$ was considered to be significant. All data are presented in the text and figures as the mean ± S.D.

Results

Identification of genes up-regulated by MK-4 in osteoblastic cells by microarray analysis

To identify up-regulated genes by MK-4 treatment in osteoblastic cells, we prepared biotin-labeled cRNA samples from MG63 cells expressing empty Flag-pcDNA3 (MG63/vector) or Flag-VP16C-SXR (MG63/Flag-VP16C-SXR) treated with vehicle (0·1% ethanol) or MK-4 (10 μM). The Affymetrix U133A GeneChip array represents more than 18 000 human transcripts from ~14 000 genes. Gene expression analysis for the MG63 samples was performed by hybridizing aliquots of cRNA (10 μg each) to the GeneChip arrays. Eighty-five transcripts were induced twofold or greater by MK-4 in MG63/vector cells, whereas 77 transcripts were induced in MG63/Flag-VP16C-SXR cells. In the present study, we focused on the SXR-independent gene expression in osteoblastic cells, by screening the common up-regulated genes (greater than or equal to twofold) in both vector and Flag-VP16C-SXR-transfected MG63 cells. In this population, we excluded genes up-regulated with the ratios of fold change in Flag-VP16C-SXR cells versus vector cells by ≥1·5-fold, as we considered that such genes were SXR dependent.

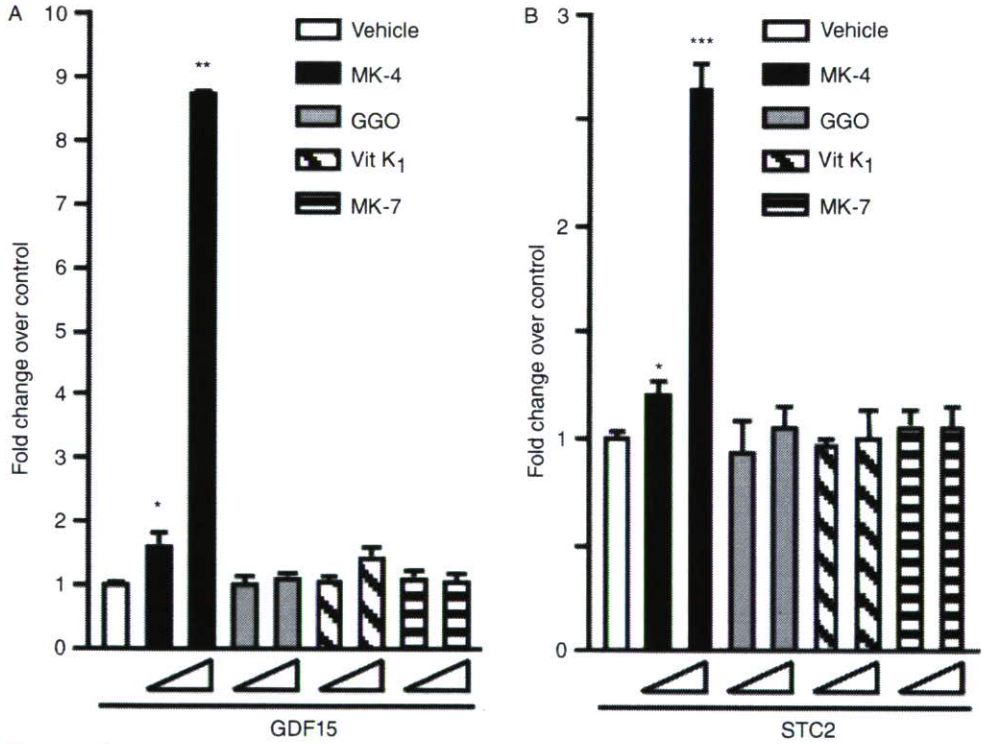

Figure 2 Specificity of MK-4 for induction of GDF15 and STC2 mRNA expression in osteoblastic cells. MG63 cells were treated with 5 or 10 μM of vitamin K_1, MK-4, MK-7, or geranylgeraniol (GGO) for 72 h. mRNA levels for GDF15 (A) and STC2 (B) were determined by qRT-PCR. Data are representative of experiments with similar results, each performed in triplicate. $^*P<0{\cdot}05$, $^{**}P<0{\cdot}01$, $^{***}P<0{\cdot}001$ when compared with control cells treated with vehicle.

Flag-VP16C-SXR was constructed previously that could provide more intense SXR ligand-dependent signals when compared with the original SXR plasmid (Ichikawa *et al.* 2006). We used Flag-VP16C-SXR as it was useful to exclude SXR-dependent genes from the SXR-independent gene group. Through this procedure, 15 transcripts from 14 distinct genes were selected as MK-4 targets that were potentially independent of SXR pathways (Table 1). We focused on GDF15 and a secreted peptide hormone STC2 as putative bone-related genes for further experiments.

Induction of GDF15 and STC2 specifically by MK-4 in osteoblastic cells

We validated whether mRNA expression levels for these two genes could be modulated by MK-4 in parental MG63 cells using quantitative RT-PCR (qRT-PCR) analysis. In proliferating culture of MG63 cells, the significant induction of both GDF15 and STC2 was detected after 48-h treatment with MK-4 (Fig. 1A). GDF15 and STC2 were also induced in mouse osteoblastic MC3T3-E1 cells after 48-h treatment with MK-4 (Fig. 1B).

We next investigated whether GDF15 and STC2 were induced by other vitamin Ks or the MK-4 side chain structure GGO. Induction of GDF15 and STC2 mRNA by vitamin K_1, MK-7, or GGO was compared with that by MK-4. MK-4 of 5 and 10 μM significantly up-regulated the *MK-4* target genes, whereas the others had no effect (Fig. 2).

Up-regulation of *MK-4* target genes in a GGCX and SXR-independent manner

Since *MK-4* target genes were not induced by vitamin K_1 or MK-7, we next sought to verify that a GGCX-mediated pathway does not participate in the induction of these *MK-4* target genes. We investigated the effects of a siRNA against GGCX on the ligand-dependent induction of gene expression. Ninety-six-hour treatment with the specific siRNA duplex against GGCX (70 nM), but not with a control siRNA directed against luciferase, reduced the GGCX mRNA level by more than 80% in MG63 cells (Fig. 3A). In that cell system, the GGCX siRNA had no effects in MK-4-activated mRNA expression for GDF15 and STC2 (Fig. 3B). We next examined whether the SXR pathway was involved in the regulation of GDF15 and STC2 mRNA expression using MG63/Flag-VP16C-SXR cells. In cells stably expressing SXR, mRNA encoding the *SXR* target gene *CYP3A4* was induced in 24 h by treatment with MK-4 or the SXR agonist RIF. In contrast, GDF15 and STC2 were up-regulated after 48-h treatment with MK-4 but not with RIF (Fig. 4A and B).

PKA is an activator for the induction of *MK-4* target genes in osteoblastic cells

It has been shown that the modulation of transcriptional activities by PKA phosphorylation is one of the key events in osteoblasts, such as through parathyroid hormone or β2-adrenergic receptor pathways (Selvamurugan *et al.* 2000, Elefteriou *et al.* 2005). There is a report that MK-4 might modulate gene expression and activate transcriptional factor activities in a PKA-dependent manner in a hepatocellular carcinoma cell line (Otsuka *et al.* 2004). Thus, we questioned whether PKA activity was responsible for the up-regulation of GDF15 and STC2 by MK-4 in osteoblastic cells. MK-4 (10 μM) markedly induced phosphorylation of PKA in MG63 cells from 2 to 24 h after the stimulation (Fig. 5A). In experiments of PKA activation by FSK (10 nM), the mRNA expression of GDF15 and STC2 was significantly up-regulated after 48-h treatment (Fig. 5B).

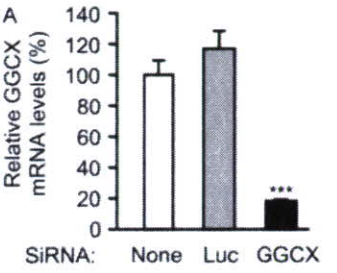

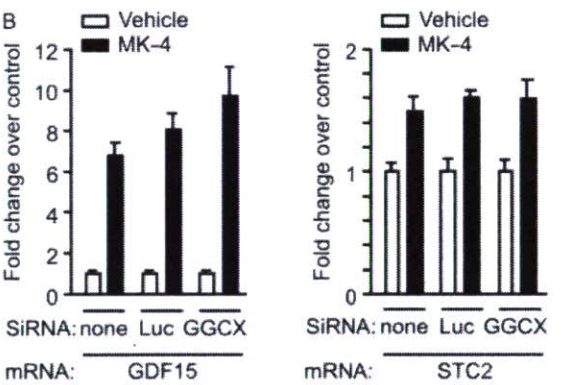

Figure 3 GDF15 and STC2 were up-regulated by a GGCX-independent pathway in osteoblastic cells. (A) MG63 cells were transfected with GGCX siRNA (70 nM) for 96 h, and mRNA expression of GGCX was determined by qRT-PCR. Data represent percentages of mRNA levels using the value with Luc siRNA treatment as 100%. (B) Effects of GGCX siRNA on MK-4-induced up-regulation of GDF15 and STC2. At 24 h after transfection of GGCX siRNA, MG63 cells were treated with MK-4 (10 μM) for 72 h and mRNA expression was determined by qRT-PCR. Data represent fold changes in mRNA over vehicle treatment. ***$P<0{\cdot}001$ when compared with control cells with no siRNA treatment.

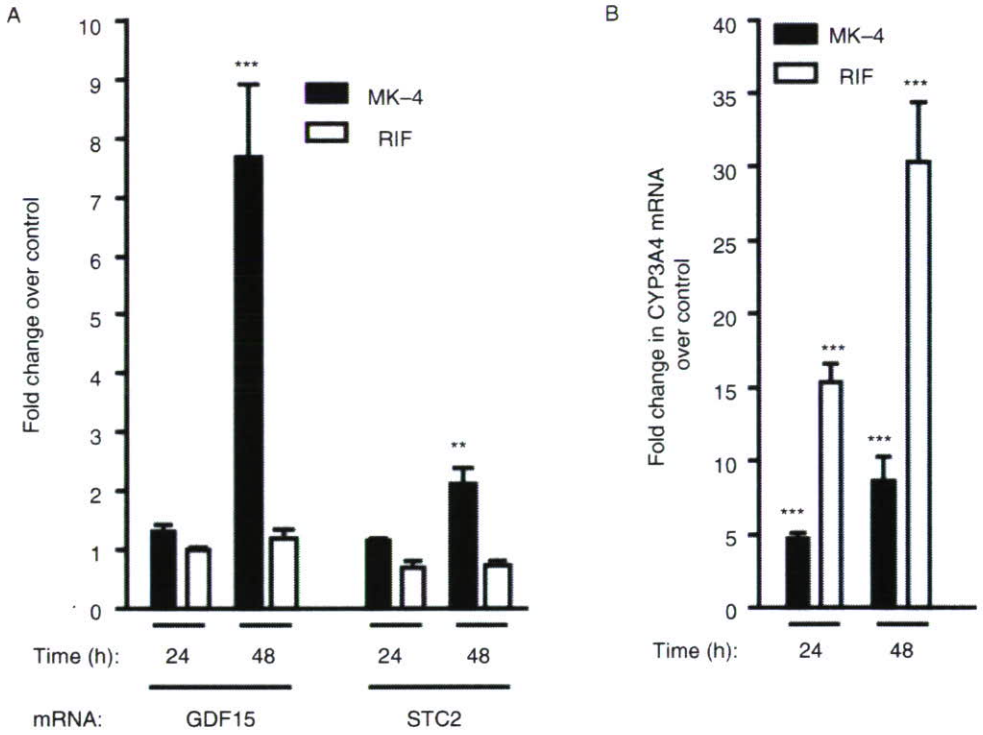

Figure 4 GDF15 and STC2 were up-regulated in an SXR-independent manner in osteoblastic cells. MG63/Flag-VP16C-SXR cells were treated with MK-4 (10 μM), rifampicin (RIF, 10 μM), or vehicle for 24 or 48 h, and mRNA expression was determined by qRT-PCR. (A) GDF15 and STC2 mRNA levels. (B) CYP3A4 mRNA levels. Data are representative of experiments with similar results, each performed in triplicate. $^{**}P<0{\cdot}01$, $^{***}P<0{\cdot}001$ when compared with control cells treated with vehicle.

Because it was likely that PKA activity was related to the transcriptional regulation of GDF15 and STC2, we further investigated whether the loss of function of PKA might affect the expression of GDF15 and STC2. Using a specific PKA inhibitor H89 (10 μM) for 72 h, MK-4-dependent up-regulation of these two genes was reduced by ~30% (Fig. 6A). We also performed the knockdown study of PRKACA in MG63 cells using a specific siRNA duplex (Fig. 6B and C). In a condition of >60% reduction of PRKACA mRNA levels by siPKA compared with the control siRNA against luciferase, MK-4-dependent up-regulation of GDF15 and STC2 was reduced by 45 and 30% respectively.

Discussion

We previously reported that SXR mediated the transcriptional regulation of several osteoblastic marker genes by the vitamin K_2 congener MK-4 (Tabb *et al.* 2003). In the present study, we identified GDF15 and STC2 as novel vitamin K_2 target genes up-regulated only by MK-4 in an SXR-independent manner in osteoblastic cells. The expression of both *GDF15* and *STC2* genes was markedly induced by MK-4 after 48-h treatment, whereas vitamin K_1, MK-7, GGO, and the SXR agonist RIF were not effective in inducing the expression of the genes. Furthermore, siRNA against GGCX did not affect the up-regulation of *GDF15* and *STC2* gene expression by MK-4. These results suggested that induction of GDF15 and STC2 was specific for MK-4 in osteoblastic cells, and that this induction was mediated by SXR- and GGCX-independent pathway(s).

GDF15 belongs to the superfamily of transforming growth factor-β, and it is generated as a 40 kDa propeptide from which the N-terminus is cleaved and a 30 kDa disulfide-linked dimeric protein is secreted as the active form (Bootcov *et al.* 1997). It was first named macrophage-inhibiting cytokine 1 (Bootcov *et al.* 1997) or placental bone morphogenetic protein (Hromas *et al.* 1997), and also later named prostate-derived factor (Paralkar *et al.* 1998) or non-steroidal anti-inflammatory drug-activated gene (Baek *et al.* 2001). GDF15 is abundantly expressed in placenta and mildly expressed in liver and prostate at baseline, but many tissues show the dramatic induction of expression following various stimuli such as cytokine, growth factor, or hypoxia (Bootcov *et al.* 1997, Albertoni *et al.* 2002, Nazarova *et al.* 2004, Schlittenhardt *et al.* 2004). It has been shown that several kinases and transcriptional factors may contribute to the regulation of GDF15

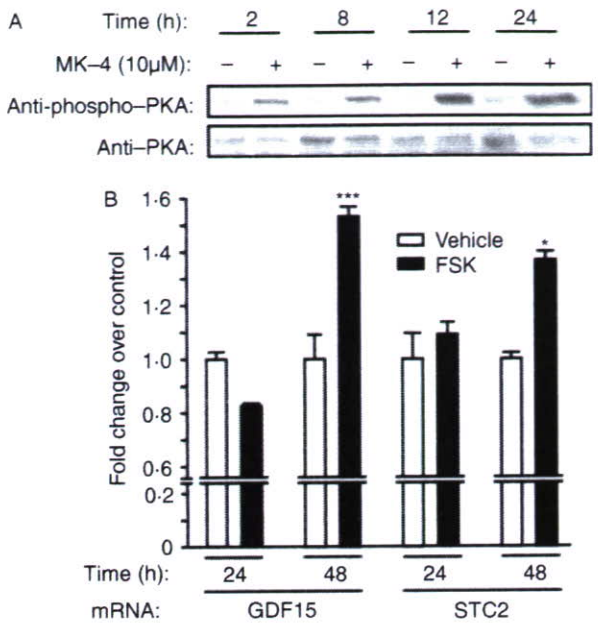

Figure 5 Phosphorylation of protein kinase A (PKA) by MK-4 and induction of GDF15 and STC2 mRNA by a PKA activator. (A) MG63 cells were treated with MK-4 (10 μM) or vehicle (MK-4,) for the indicated times. Whole cell lysates were separated by SDS-PAGE, and phosphorylated PKA was detected by immunoblot analysis using anti-phospho-PKA antibody. The identical membrane was re-probed with whole PKA antibody (anti-PKA). (B) MG63 cells were treated with forskolin (FSK, 10 nM) or vehicle (0·1% DMSO) for the indicated times. mRNA levels for GDF15 and STC2 were determined by qRT-PCR. Data are representative of experiments with similar results, each performed in triplicate. $^{*}P<0{\cdot}05$, $^{***}P<0{\cdot}001$ when compared with control cells treated with vehicle.

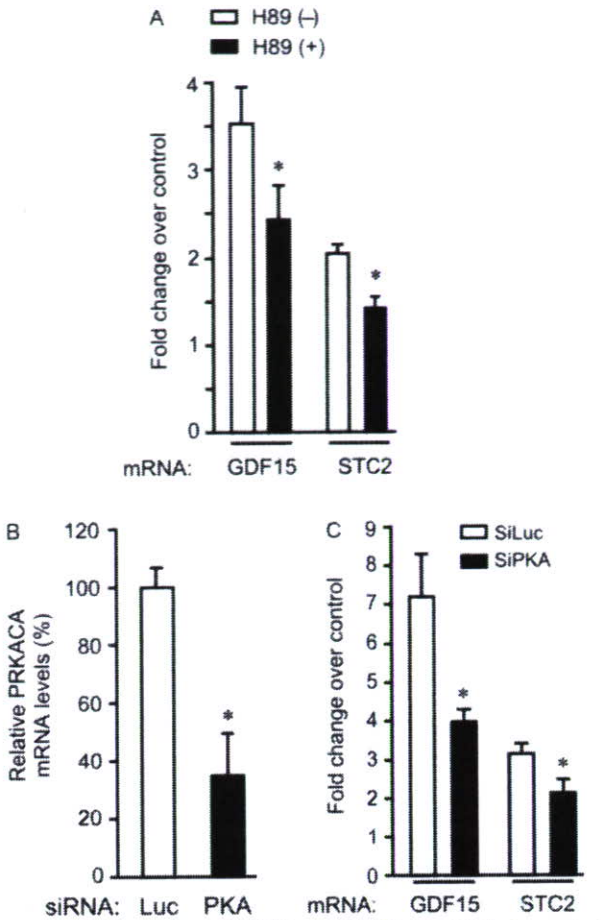

Figure 6 MK-4 induces GDF15 and STC2 in a PKA-dependent manner. (A) MG63 cells were treated with MK-4 (10 μM) or vehicle in the presence or absence of H89 (10 μM) for 72 h. mRNA levels for GDF15 and STC2 were determined by qRT-PCR. (B) MG63 cells were transfected with siRNAs (14 nM) that target either α-catalytic subunit of PKA, PRKACA (siPKA), or luciferase (siLuc) for 72 h. PRKACA mRNA expression was determined by qRT-PCR. (C) Effects of siPKA on MK-4-dependent up-regulation of GDF15 and STC2. Cells were transfected with siRNAs (14 nM) and incubated with MK-4 (10 μM) or vehicle for 72 h. Data are representative of experiments with similar results, each performed in triplicate. $^{*}P<0{\cdot}05$ when compared with control cells treated with vehicle test.

expression, including p53 (Li *et al.* 2000, Tan *et al.* 2000), protein kinase C (Shim & Eling 2005), phosphatidylinositol 3-kinase/AKT (Yamaguchi *et al.* 2004), or early growth response 1 (EGR-1; Baek *et al.* 2005). The transcriptional regulation by PKA has not been definitely shown previously, yet it is likely that PKA is involved in GDF15 regulation as the gene expression was induced by dibutyryl cAMP in murine preadipocytes (Uldry *et al.* 2006). Although PKA sometimes phosphorylates p53, it is unlikely that p53 is responsible for the modulation of GDF15 expression in MG63 cells as the cell line has been shown to lack p53 (Masuda *et al.* 1987, Diller *et al.* 1990).

Regarding the physiological significance of GDF15 in bone-related tissues, the gene may play a role in the developmental stage as it has been shown to be expressed in the skin and in the cartilaginous tissue in the 18-dpc rat embryos (Paralkar *et al.* 1998). Similar to the function of bone morphogenic proteins, s.c. implantation of recombinant GDF15 protein ectopically induced the cartilage and immature endochondral bone formation (Paralkar *et al.* 1998). In prostate cancer, GDF15 expression was expressed only in osseous metastatic lesions, while it was reduced or absent in primary tumor, suggesting that GDF15 expression might be linked to the osteoblastic phenomena associated with bone metastasis (Thomas *et al.* 2001). GDF15 also has modulating effects on cell adhesion or proliferation (Li *et al.* 2000, Tan *et al.* 2000, Nazarova *et al.* 2004). As MK-4 has been known as a modulator of cell proliferation in osteoblastic cells (Akedo *et al.* 1992) and hepatocellular carcinoma cells (Otsuka *et al.* 2004), GDF15 might be also involved in this growth-regulatory function of MK-4.

STCs represent a small family of secreted glycoprotein hormones, consisting of STC1 and STC2, which has been conserved from fish to mammals. It was assumed that mammalian STC would mimic the function of fish STC-1 in mineral homeostasis (Olsen

et al. 1996, Wagner *et al.* 1997, Madsen *et al.* 1998). STC1 is expressed in osteoblastic cells and could be induced during osteoblastic differentiation of rat fetal calvaria cells (Yoshiko *et al.* 1999, 2003). Overexpression and knockdown study of STC1 led to the acceleration and retardation of osteogenic development respectively (Yoshiko *et al.* 2003). STC1 is also expressed in chondrocytes and may also stimulate chondrocyte proliferation in cartilage matrix (Jiang *et al.* 2000, Filvaroff *et al.* 2002). In transgenic mice expressing human STC2, growth restriction and developmental retardation were observed in both prenatal and postnatal stages, and ossification was reduced in different endochondral skeletal elements (Gagliardi *et al.* 2005). Systemic overexpression of human STC1 in transgenic mice, however, also exhibited postnatal growth retardation (Varghese *et al.* 2002) and reduced ossification in cranial bones (Gagliardi *et al.* 2005), suggesting the discrepancy between animal models and culture cells. More specific studies targeting osteoblast and chondrocyte lineage will be required for better understanding of the STC physiology in bone development and formation, yet STC could be one of the key factors for the regulation of bone homeostasis. Interestingly, it has been shown that STC2 is closely related to steroid hormone physiology, as its expression is induced by estrogen (Charpentier *et al.* 2000, Bouras *et al.* 2002), or it has an inhibitory effect on FSH-induced progesterone production in rat ovary granulose cells (Luo *et al.* 2005). It is likely that STC2 could play a paracrine role also in bone formation.

In this study, we investigated the effects of PKA on GDF15 and STC2 expression in osteoblastic cells and demonstrated that PKA was responsible, at least in part, for the MK-4-dependent up-regulation of these two genes. It has been reported that MK-4 activated transcriptional factors activating enhancer-binding protein 2α (AP-2), upstream stimulatory factor (USF), and cyclic adenosine monophosphate response element-binding protein (CREB), and PKA activity might be stimulated by MK-4 in hepatocellular carcinoma cell line HepG2 (Otsuka *et al.* 2004). The activation of PKA by FSK in the present study mimicked the MK-4-induced up-regulation of GDF15 and STC2 in osteoblastic cells, although it is not clear whether MK-4 directly increases cyclic AMP production. It is also possible that PKA is phosphorylated by MK-4 through a cAMP-independent pathway, such as the one mediated by sphingosine (Ma *et al.* 2005). Future study will reveal the molecular details of MK-4-induced PKA activity in osteoblastic cells. It might be also interesting to investigate whether the MK-4-dependent PKA activation is important in other non-osteoblastic cells.

Here, we have shown that the PKA-dependent pathway is involved in the regulation of *MK-4* target genes in osteoblastic cells in an SXR- and GGCX-independent manner. Our data suggest that GDF15 and STC2 are novel *MK-4* target genes up-regulated by the PKA-dependent pathway. Induction of GDF15 and STC2 at proliferation stage and post-confluent phase in osteoblastic cells might affect osteogenesis and chondrogenesis via autocrine or paracrine mechanisms.

Acknowledgements

We thank T Suzuki and R Nozawa for their technical assistance. This work was supported in part by grants-in-aid from the Ministry of Health, Labor and Welfare, the Promotion and Mutual Aid Corporation for Private Schools of Japan, the Japan Society for the Promotion of Science, and the NIH (GM-60572 to BB). This work was supported in part by a grant of the Genome Network Project from the Ministry of Education, Culture, Sports, Science and Technology of Japan. The authors declare that there is no conflict of interest that would prejudice the impartiality of this scientific work.

Disclosure

The authors have nothing to declare.

References

Akedo Y, Hosoi T, Inoue S, Ikegami A, Mizuno Y, Kaneki M, Nakamura T, Ouchi Y & Orimo H 1992 Vitamin K_2 modulates proliferation and function of osteoblastic cells in vitro. *Biochemical and Biophysical Research Communications* **187** 814–820.

Albertoni M, Shaw PH, Nozaki M, Godard S, Tenan M, Hamou MF, Fairlie DW, Breit SN, Paralkar VM, de Tribolet N *et al.* 2002 Anoxia induces macrophage inhibitory cytokine-1 (MIC-1) in glioblastoma cells independently of p53 and HIF-1. *Oncogene* **21** 4212–4219.

Baek SJ, Kim KS, Nixon JB, Wilson LC & Eling TE 2001 Cyclooxygenase inhibitors regulate the expression of a TGF-β superfamily member that has proapoptotic and antitumorigenic activities. *Molecular Pharmacology* **59** 901–908.

Baek SJ, Kim JS, Moore SM, Lee SH, Martinez J & Eling TE 2005 Cyclooxygenase inhibitors induce the expression of the tumor suppressor gene *EGR-1*, which results in the up-regulation of NAG-1, an antitumorigenic protein. *Molecular Pharmacology* **67** 356–364.

Bootcov MR, Bauskin AR, Valenzuela SM, Moore AG, Bansal M, He XY, Zhang HP, Donnellan M, Mahler S, Pryor K *et al.* 1997 MIC-1, a novel macrophage inhibitory cytokine, is a divergent member of the TGF-β superfamily. *PNAS* **94** 11514–11519.

Booth SL, Tucker KL, Chen H, Hannan MT, Gagnon DR, Cupples LA, Wilson PW, Ordovas J, Schaefer EJ, Dawson-Hughes B *et al.* 2000 Dietary vitamin K intakes are associated with hip fracture but not with bone mineral density in elderly men and women. *American Journal of Clinical Nutrition* **71** 1201–1208.

Bouras T, Southey MC, Chang AC, Reddel RR, Willhite D, Glynne R, Henderson MA, Armes JE & Venter DJ 2002 *Stanniocalcin 2* is an estrogen-responsive gene coexpressed with the estrogen receptor in human breast cancer. *Cancer Research* **62** 1289–1295.

Charpentier AH, Bednarek AK, Daniel RL, Hawkins KA, Laflin KJ, Gaddis S, MacLeod MC & Aldaz CM 2000 Effects of estrogen on global gene expression: identification of novel targets of estrogen action. *Cancer Research* **60** 5977–5983.

Diller L, Kassel J, Nelson CE, Gryka MA, Litwak G, Gebhardt M, Bressac B, Ozturk M, Baker SJ, Vogelstein B *et al.* 1990 p53 functions as a cell cycle control protein in osteosarcomas. *Molecular and Cellular Biology* **10** 5772–5781.

Elefteriou F, Ahn JD, Takeda S, Starbuck M, Yang X, Liu X, Kondo H, Richards WG, Bannon TW, Noda M *et al.* 2005 Leptin regulation of bone resorption by the sympathetic nervous system and CART. *Nature* **434** 514–520.

Filvaroff EH, Guillet S, Zlot C, Bao M, Ingle G, Steinmetz H, Hoeffel J, Bunting S, Ross J, Carano RA *et al.* 2002 Stanniocalcin 1 alters muscle and bone structure and function in transgenic mice. *Endocrinology* **143** 3681–3690.

Gagliardi AD, Kuo EY, Raulic S, Wagner GF & DiMattia GE 2005 Human stanniocalcin-2 exhibits potent growth-suppressive properties in transgenic mice independently of growth hormone and IGFs. *American Journal of Physiology. Endocrinology and Metabolism* **288** E92–E105.

Hromas R, Hufford M, Sutton J, Xu D, Li Y & Lu L 1997 PLAB, a novel placental bone morphogenetic protein. *Biochimica et Biophysica Acta* **1354** 40–44.

Ichikawa T, Horie-Inoue K, Ikeda K, Blumberg B & Inoue S 2006 Steroid and xenobiotic receptor SXR mediates vitamin K_2-activated transcription of extracellular matrix-related genes and collagen accumulation in osteoblastic cells. *Journal of Biological Chemistry* **281** 16927–16934.

Jiang WQ, Chang AC, Satoh M, Furuichi Y, Tam PP & Reddel RR 2000 The distribution of stanniocalcin 1 protein in fetal mouse tissues suggests a role in bone and muscle development. *Journal of Endocrinology* **165** 457–466.

Li PX, Wong J, Ayed A, Ngo D, Brade AM, Arrowsmith C, Austin RC & Klamut HJ 2000 Placental transforming growth factor-beta is a downstream mediator of the growth arrest and apoptotic response of tumor cells to DNA damage and p53 overexpression. *Journal of Biological Chemistry* **275** 20127–20135.

Luo G, Ducy P, McKee MD, Pinero GJ, Loyer E, Behringer RR & Karsenty G 1997 Spontaneous calcification of arteries and cartilage in mice lacking matrix GLA protein. *Nature* **386** 78–81.

Luo CW, Pisarska MD & Hsueh AJ 2005 Identification of a stanniocalcin paralog, stanniocalcin-2, in fish and the paracrine actions of stanniocalcin-2 in the mammalian ovary. *Endocrinology* **146** 469–476.

Ma Y, Pitson S, Hercus T, Murphy J, Lopez A & Woodcock J 2005 Sphingosine activates protein kinase A type II by a novel cAMP-independent mechanism. *Journal of Biological Chemistry* **280** 26011–26017.

Madsen KL, Tavernini MM, Yachimec C, Mendrick DL, Alfonso PJ, Buergin M, Olsen HS, Antonaccio MJ, Thomson AB & Fedorak RN 1998 Stanniocalcin: a novel protein regulating calcium and phosphate transport across mammalian intestine. *American Journal of Physiology* **274** G96–G102.

Masuda H, Miller C, Koeffler HP, Battifora H & Cline MJ 1987 Rearrangement of the *p53* gene in human osteogenic sarcomas. *PNAS* **84** 7716–7719.

Nazarova N, Qiao S, Golovko O, Lou YR & Tuohimaa P 2004 Calcitriol-induced prostate-derived factor: autocrine control of prostate cancer cell growth. *International Journal of Cancer* **112** 951–958.

Nishimoto SK & Price PA 1985 The vitamin K-dependent bone protein is accumulated within cultured osteosarcoma cells in the presence of the vitamin K antagonist warfarin. *Journal of Biological Chemistry* **260** 2832–2836.

Olsen HS, Cepeda MA, Zhang QQ, Rosen CA & Vozzolo BL 1996 Human stanniocalcin: a possible hormonal regulator of mineral metabolism. *PNAS* **93** 1792–1796.

Otsuka M, Kato N, Shao RX, Hoshida Y, Ijichi H, Koike Y, Taniguchi H, Moriyama M, Shiratori Y, Kawabe T *et al.* 2004 Vitamin K_2 inhibits the growth and invasiveness of hepatocellular carcinoma cells via protein kinase A activation. *Hepatology* **40** 243–251.

Paralkar VM, Vail AL, Grasser WA, Brown TA, Xu H, Vukicevic S, Ke HZ, Qi H, Owen TA & Thompson DD 1998 Cloning and characterization of a novel member of the transforming growth factor-β/bone morphogenetic protein family. *Journal of Biological Chemistry* **273** 13760–13767.

Schlittenhardt D, Schober A, Strelau J, Bonaterra GA, Schmiedt W, Unsicker K, Metz J & Kinscherf R 2004 Involvement of growth differentiation factor-15/macrophage inhibitory cytokine-1 (GDF-15/MIC-1) in oxLDL-induced apoptosis of human macrophages *in vitro* and in arteriosclerotic lesions. *Cell and Tissue Research* **318** 325–333.

Selvamurugan N, Pulumati MR, Tyson DR & Partridge NC 2000 Parathyroid hormone regulation of the rat collagenase-3 promoter by protein kinase A-dependent transactivation of core binding factor α1. *Journal of Biological Chemistry* **275** 5037–5042.

Shanahan CM & Weissberg PL 1998 Smooth muscle cell heterogeneity: patterns of gene expression in vascular smooth muscle cells *in vitro* and *in vivo*. *Arteriosclerosis, Thrombosis, and Vascular Biology* **18** 333–338.

Shim M & Eling TE 2005 Protein kinase C-dependent regulation of NAG-1/placental bone morphogenic protein/MIC-1 expression in LNCaP prostate carcinoma cells. *Journal of Biological Chemistry* **280** 18636–18642.

Shiraki M, Shiraki Y, Aoki C & Miura M 2000 Vitamin K_2 (menatetrenone) effectively prevents fractures and sustains lumbar bone mineral density in osteoporosis. *Journal of Bone and Mineral Research* **15** 515–521.

Tabb MM, Sun A, Zhou C, Grun F, Errandi J, Romero K, Pham H, Inoue S, Mallick S, Lin M *et al.* 2003 Vitamin K_2 regulation of bone homeostasis is mediated by the steroid and xenobiotic receptor SXR. *Journal of Biological Chemistry* **278** 43919–43927.

Tan M, Wang Y, Guan K & Sun Y 2000 PTGF-β, a type β transforming growth factor (TGF-β) superfamily member, is a *p53* target gene that inhibits tumor cell growth via TGF-β signaling pathway. *PNAS* **97** 109–114.

Thomas R, True LD, Lange PH & Vessella RL 2001 Placental bone morphogenetic protein (*PLAB*) gene expression in normal, pre-malignant and malignant human prostate: relation to tumor development and progression. *International Journal of Cancer* **93** 47–52.

Uldry M, Yang W, St-Pierre J, Lin J, Seale P & Spiegelman BM 2006 Complementary action of the PGC-1 coactivators in mitochondrial biogenesis and brown fat differentiation. *Cell Metabolism* **3** 333–341.

Varghese R, Gagliardi AD, Bialek PE, Yee SP, Wagner GF & Dimattia GE 2002 Overexpression of human stanniocalcin affects growth and reproduction in transgenic mice. *Endocrinology* **143** 868–876.

Vergnaud P, Garnero P, Meunier PJ, Breart G, Kamihagi K & Delmas PD 1997 Undercarboxylated osteocalcin measured with a specific immunoassay predicts hip fracture in elderly women: the EPIDOS Study. *Journal of Clinical Endocrinology and Metabolism* **82** 719–724.

Wagner GF, Vozzolo BL, Jaworski E, Haddad M, Kline RL, Olsen HS, Rosen CA, Davidson MB & Renfro JL 1997 Human stanniocalcin inhibits renal phosphate excretion in the rat. *Journal of Bone and Mineral Research* **12** 165–171.

Yamaguchi K, Lee SH, Eling TE & Baek SJ 2004 Identification of nonsteroidal anti-inflammatory drug-activated gene (*NAG-1*) as a novel downstream target of phosphatidylinositol 3-kinase/AKT/GSK-3beta pathway. *Journal of Biological Chemistry* **279** 49617–49623.

Yoshiko Y, Son A, Maeda S, Igarashi A, Takano S, Hu J & Maeda N 1999 Evidence for stanniocalcin gene expression in mammalian bone. *Endocrinology* **140** 1869–1874.

Yoshiko Y, Maeda N & Aubin JE 2003 Stanniocalcin 1 stimulates osteoblast differentiation in rat calvaria cell cultures. *Endocrinology* **144** 4134–4143.

Received in final form 28 June 2007
Accepted 30 July 2007
Made available online as an Accepted Preprint 2 August 2007

SPINE Volume 32, Number 1, pp 25–29

Q89R Polymorphism in the LDL Receptor-Related Protein 5 Gene Is Associated With Spinal Osteoarthritis in Postmenopausal Japanese Women

Tomohiko Urano, MD, PhD,* Masataka Shiraki, MD, PhD,† Ken'ichiro Narusawa, MD, PhD,‡ Takahiko Usui, MD,* Noriko Sasaki, BS,* Takayuki Hosoi, MD, PhD,§ Yasuyoshi Ouchi, MD, PhD,* Toshitaka Nakamura, MD, PhD,‡ and Satoshi Inoue, MD, PhD,*‖

Study Design. An association study investigating the genetic etiology for spinal osteoarthritis.

Objective. To determine the association of single-nucleotide polymorphism (SNP) causing an amino-acid change (Q89R) in the low-density lipoprotein receptor-related protein 5 (LRP5) coding region with spinal osteoarthritis.

Summary of Background Data. Wnt/β-catenin signaling pathway regulates bone density through a Wnt coreceptor LRP5. This pathway is also involved in cartilage development and homeostasis, suggesting that genetic variation in LRP5 gene may affect the pathogenesis of cartilage-related diseases, such as osteoarthritis.

Methods. We evaluated the presence of osteophytes, endplate sclerosis, and narrowing of disc spaces in 357 Japanese postmenopausal women. Missense coding SNP for Q89R of LRP5 gene was determined using TaqMan polymerase chain reaction (PCR) method.

Results. We found that subjects without the R allele (QQ; n = 321) had a significantly lower osteophyte formation score than did subjects bearing at least one R allele (QR + RR; n = 36) (7.80 *vs.* 10.89, $P = 0.0019$ by analysis of covariance).

Conclusions. We suggest that a genetic variation at the LRP5 gene locus is associated with spinal osteoarthritis, in line with the involvement of the LRP5 gene in the bone and cartilage metabolism.

Key words: single-nucleotide polymorphism (SNP), low-density lipoprotein receptor-related protein 5 (LRP5), spinal osteoarthritis, osteophytosis. **Spine 2007;32:25–29**

Osteoarthritis of the spine is a very common condition in the axial skeletons of aged people.[1] Vertebral osteophytes, endplate sclerosis, and intervertebral disc narrowing are recognized as characteristic features of spinal degeneration. Recent studies indicate that the appearance of these radiographic features is influenced by genetic factors, physical loading, and other environmental factors.[2,3] Association studies in using various definitions of osteoarthritis have been performed, mainly investigating genes encoding structural proteins of the extracellular matrix of cartilage (*e.g.*, collagen Type II α1, cartilage matrix protein, and aminoguanidine) or genes playing a role in the regulation of bone density and mass (*e.g.*, vitamin D receptor, insulin-like growth factor-I, and estrogen receptor α).[4,5]

The Wnt (wingless-type MMTV integration site family) represents a large group of secreted signaling proteins that are involved in cell proliferation, differentiation, and morphogenesis.[6] The name of "Wnt" is derived from wingless gene in *Drosophila melanogaster*[7] and murine int-1 oncogene identified in tumors induced by mouse mammary tumor virus.[8] It is also known that Wnt and bone morphogenetic protein (BMP) signals control apical ectodermal ridge formation and dorsal-ventral patterning during limb development.[9,10] Wnt proteins activate signal transduction through Frizzled, which act as receptors for Wnt proteins[11] and induce stabilization of cytoplasmic β-catenin protein, which also regulates target gene expression as a transcriptional coactivator. The physiologic role of Wnt in the regulation of osteoblastogenesis has been studied in experimental models, in embryonic mesenchymal progenitor cells expressing Wnt3a[12] or in mice expressing Wnt10b transgene in bone marrow.[13] It is also shown that activated β-catenin modulate osteoblast and chondrocyte differentiation.[14,15] Meanwhile, LDL receptor-related protein 5 and 6 (LRP5/6) were also found to be required for Wnt coreceptors.[16,17] Recent reports demonstrated that the Wnt/β-catenin signaling pathway regulates bone density through LRP5.[18–21] These findings indicate that Wnt-β-catenin signaling pathway plays important roles in the skeletal biology.

In addition to the regulation of limb development and bone metabolism, Wnt/β-catenin signaling may be involved in maintenance and pathophysiology of cartilage. This possibility is indirectly supported by the observation that several Wnt proteins and Frizzled receptors are expressed in synovial tissue of arthritic cartilage.[22] In

From the *Department of Geriatric Medicine, Graduate School of Medicine, The University of Tokyo, Tokyo, Japan; †Research Institute and Practice for Involutional Diseases, Nagano, Japan; ‡Department of Orthopedic Surgery, University of Occupational and Environmental Health, School of Medicine, Kitakyushu, Japan; §Department of Advanced Medicine, National Center for Geriatrics and Gerontology, Aichi, Japan; and ‖Research Center for Genomic Medicine, Saitama Medical School, Saitama, Japan.

Acknowledgment date: October 28, 2005. First revision date: February 23, 2006. Acceptance date: March 2, 2006.

Supported in part by grants from the Japanese Ministry of Health, Labor, Welfare and Japan Society for the Promotion of Science and by a grant of the Genome Network Project from the Ministry of Culture, Education, Sports, Science and Technology of Japan.

The manuscript submitted does not contain information about medical device(s)/drug(s).

No funds were received in support of this work. No benefits in any form have been or will be received from a commercial party related directly or indirectly to the subject of this manuscript.

Address correspondence and reprint requests to Satoshi Inoue, MD, PhD, Department of Geriatric Medicine, Graduate School of Medicine, University of Tokyo, 7-3-1, Hongo, Bumkyo-ku, Tokyo, Japan; E-mail: INOUE-GER@h.u-tokyo.ac.jp

addition, a secreted Frizzled-related protein (FrzB-2) that act as an antagonist for Frizzled receptor is strongly expressed in osteoarthritic cartilage and may regulate chondrocyte apoptosis.[23] It is also reported that chondrocytes express β-catenin at a low level and accumulation of β-catenin is sufficient to cause dedifferentiation of chondrocytes, suggesting that Wnt signaling is involved in cartilage metabolism.[24] Thus, it is assumed that LRP5 modulates Wnt/β-catenin signaling pathway in the bone and cartilage homeostasis. In the present study, we examine an association between a polymorphism in LRP5 gene and radiographic features of spinal osteoarthritis, including osteophyte formation, endplate sclerosis, and disc space narrowing number to investigate a possible contribution of LRP5 to human bone and cartilage metabolism.

■ Materials and Methods

Subjects. Genotypes were analyzed in DNA sample obtained from 357 healthy postmenopausal Japanese women (mean age ± SD; 65.22 ± 8.20 years) living in central area of Japan. Exclusion criteria included endocrine disorders such as hyperthyroidism, hyperparathyroidism, diabetes mellitus, liver disease, renal disease, use of medications known to affect bone metabolism (*e.g.*, corticosteroids, anticonvulsants, heparin sodium), or unusual gynecologic history. Patients with severe hip and knee arthritis were excluded from the present study. The eligibility of subjects was determined by taking history-physical examination. All were nonrelated volunteers and provided informed consent before this study. Ethical approval for the study was obtained from appropriate ethics committees.

Radiographic Grading of Osteoarthritis of the Spine. Conventional thoracic and lumbar spinal plain roentgenograms in lateral and anteroposterior projection were obtained from all participants. The severities of spinal degeneration, including osteophyte formation, endplate sclerosis, and disc space narrowing, were assessed semiquantitatively from T4–T5 to L4–L5 disc level or from T4 to L5 vertebrae by using the grading scale of Yu *et al.*[25] Briefly, osteophyte formation at a given disc was graded 0° to 3°, endplate sclerosis at given vertebra was graded 0° to 2°, and disc space narrowing was graded 0° to 1°. Then we defined sum of each degree from T4–T5 to L4–L5 disc level for osteophyte formation on anteroposterior radiographs as a score of osteophyte formation. We also defined sum of each degree from T4 to L4 vertebra for endplate sclerosis and that from T4–T5 to L4–L5 disc level for disc space narrowing on lateral radiographs as a score of endplate sclerosis and disc narrowing, respectively. Then we defined sum of each 13 grade for osteophyte formation on anteroposterior radiographs as a score of osteophyte formation. We also defined sum of 13 grade for endplate sclerosis and disc space narrowing on lateral radiographs as a score of endplate sclerosis and disc narrowing, respectively.

Measurement of Bone Mineral Density (BMD) and Biochemical Markers. The lumbar spine BMD and total body BMD (in g/cm^2) of each participant were measured by dual-energy radiograph absorptiometry using fast-scan mode (DPX-L; Lunar, Madison, WI). The BMD data were recorded as "Z scores," that is, deviation from the weight-adjusted average BMD for each age. Z scores were calculated using installed software (Lunar DPX-L) on the basis of data from 20,000 Japanese women.

We measured serum concentration of calcium (Ca), phosphate (P), alkaline phosphatase (ALP), intact-osteocalcin (I-OC, ELISA; Teijin, Tokyo, Japan), intact parathyroid hormone (PTH), calcitonin (CT), and 1, 25(OH)2D3. We also measured urinary ratios of urinary deoxypyridinoline (DPD, HPLC method) to creatinine.

Determination of a Single Nucleotide Polymorphism in the LRP5 Gene. DNA was extracted from peripheral leukocytes by standard techniques. Missense coding SNP for Q89R (c. 266A>G) of the LRP5 gene was determined using Assays by Design SNP Genotyping Products (Applied BioSystems) that based on the TaqMan PCR method.[26] Missense coding means that the alteration of a codon (an array of three consecutive bases in mRNA) that encodes a different amino acid. TaqMan PCR method uses two kinds of TaqMan probes that correspond to a DNA fragment including the target SNP site with different alleles and the 5′–3′ nuclease activity of Taq polymerase that is essential for PCR. TaqMan probes include fluorescence dyes at their 5′ ends and a quencher at their 3′ ends. During PCR cycles, TaqMan probes will anneal to target DNA and will be excised by the 5′–3′ nuclease activity of Taq polymerase if there is no mismatch between the probes and target sequences. Then the fluorescence dyes will be released from the probes and the intensity of fluorescence can be monitored by using ABI PRISM 7000 (Applied Biosystems) as a fluorescence detector. The allele frequencies of Q89R polymorphism were confirmed as they were not significantly deviated from Hardy-Weinberg equilibrium. Since Hardy-Weinberg equilibrium is based on the following assumptions including no genetic drift, no gene flow, no natural selection, negligible mutations, and random mating, the population under the equilibrium is not evolving and its genotype and allele frequencies are predicted to remain unchanged over successive generations. Thus, we considered that our subjects were eligible for the correlation study.

Statistical Analysis. We divided subjects into those having one or two chromosomes of the minor G-allele (QR + RR) and those with only the major A-allele (QQ) encoded at the same locus. Comparisons of Z scores of lumbar spine and biochemical markers between these two groups were subjected to statistical analysis (unpaired *t* test; StatView-J 4.5, SAS Institute Inc.). The association between these two groups and osteoarthritis parameters (number of osteophyte, endoplate sclerosis, and disc narrowing) was assessed by unpaired *t* test and by analysis of covariance (ANCOVA) with adjustment of confounding clinical variables (age, body weight, and height). A P value less than 0.05 was considered statistically significant.

■ Results

We analyzed the genotypes for the SNP of LRP5 at Q89R (c.266 A>G) in subjects, using TaqMan methods. Among 357 postmenopausal Japanese women, 321 were QQ homozygotes, 35 were QR heterozygotes, and 1 was RR homozygote. The allelic frequencies of this SNP in the present study were in Hardy-Weinberg equilibrium.

Because only 1 of these subjects carried the RR genotype of the Q89R polymorphism, we compared those who carried the R allele (QR or RR) with those who did

Table 1. Comparison of Background, Clinical Characteristics Between Subjects Bearing at Least 1 R allele (QR + RR) and Subjects With No R allele (QQ) in the *LRP5 Gene Coding Region* (Q89R)

Item	Genotype (mean ± SD) QQ	QR + RR	P
No. of subjects	321	36	
Age (yr)	65.0 ± 8.2	67.3 ± 8.0	NS
Height (cm)	150.7 ± 5.7	151.1 ± 7.1	NS
Body weight (kg)	50.5 ± 7.6	51.3 ± 7.9	NS
Lumber spine BMD (Z score)	−0.28 ± 1.40	−0.17 ± 1.89	NS
ALP (IU/L)	190.8 ± 61.3	194.8 ± 81.1	NS
I-OC (ng/mL)	8.2 ± 4.0	7.4 ± 3.0	NS
DPD (pmol/μmol of Cr)	7.6 ± 4.0	7.6 ± 2.3	NS
Intact PTH (pg/mL)	35.6 ± 16.7	34.6 ± 14.1	NS
1,25 $(OH)_2D_3$ (pg/mL)	36.1 ± 10.8	37.3 ± 14.6	NS
BMI	22.1 ± 3.0	22.8 ± 3.1	NS

BMD indicates bone mineral density; ALP, alkaline phosphatase; I-OC, intact-osteocalcin; DPD, deoxypyridinoline; PTH, parathyroid hormone; BMI, body mass index; NS, not significant. Statistical analysis was performed according to the method described in the text.

not (QQ). The lumbar BMD was not statistically different between these groups (Table 1). The background and biochemical data were not statistically different between these groups (Table 1). On ANCOVA analysis, we found significant associations between LRP5 Q89R genotype and osteophyte formation score after controlling for age, weight, and height. Women without the R allele (QQ; n = 321) had a significantly lower osteophyte formation score than did subjects bearing at least one R allele (QR + RR; n = 36) (7.80 ± 6.51 *vs.* 10.89 ± 7.6, $P = 0.0019$, Figure 1A; Table 2). We also found significant association between them on unpaired *t* test ($P = 0.0083$, Table 1). On the other hand, the occurrence of disc narrowing and endplate sclerosis did not significantly differ in those with and without at least one R allele (Figure 1B, C; Table 2).

Table 2. Association of the *LRP5* SNP Genotype

Item	Genotype (mean ± SD) QQ	QR + RR	P (unpaired *t* test)	P (ANCOVA)
No. of subjects	321	36		
Osteophyte formation score	7.80 ± 6.51	10.89 ± 7.6	0.0083	0.0019
Endoplate sclerosis score	0.368 ± 0.845	0.389 ± 0.994	NS	NS
Disc space narrowing score	2.03 ± 1.88	2.06 ± 1.84	NS	NS

ANCOVA indicates analysis of covariance; NS, not significant.

■ Discussion

The present study is the first report that shows the influence of a single-nucleotide polymorphism of LRP5 gene on spinal osteoarthritis as far as we know. Targeting the pathogenesis of low back pain, we have previously investigated associations of genetic factors with osteoporosis. LRP5 has been shown as one of the correlated genes in Japanese postmenopausal women.[27] Because spinal osteoarthritis is another major reason for low back pain, we have extended our association study of LRP5 polymorphism with spinal osteoarthritis. We demonstrated that the Japanese postmenopausal women who had one or two allele(s) of a nonsynonymous change (Q89R) in LRP5 gene showed significantly higher osteophyte formation score of spine. Our finding may also be supported by genome-wide scan for osteoarthritis-susceptibility loci that showed a linkage to chromosome 11q12-13,[28,29] which includes the LRP5 gene locus on 11q13.4. It has been recently shown that single-nucleotide polymorphisms in LRP5 gene provided no correlation with knee osteoarthritis status while haplotype analysis revealed that there was a common haplotype that provided a 1.6-fold increased risk,[30] suggesting that LRP5 might be involved in the pathogenesis of osteoarthritis also in

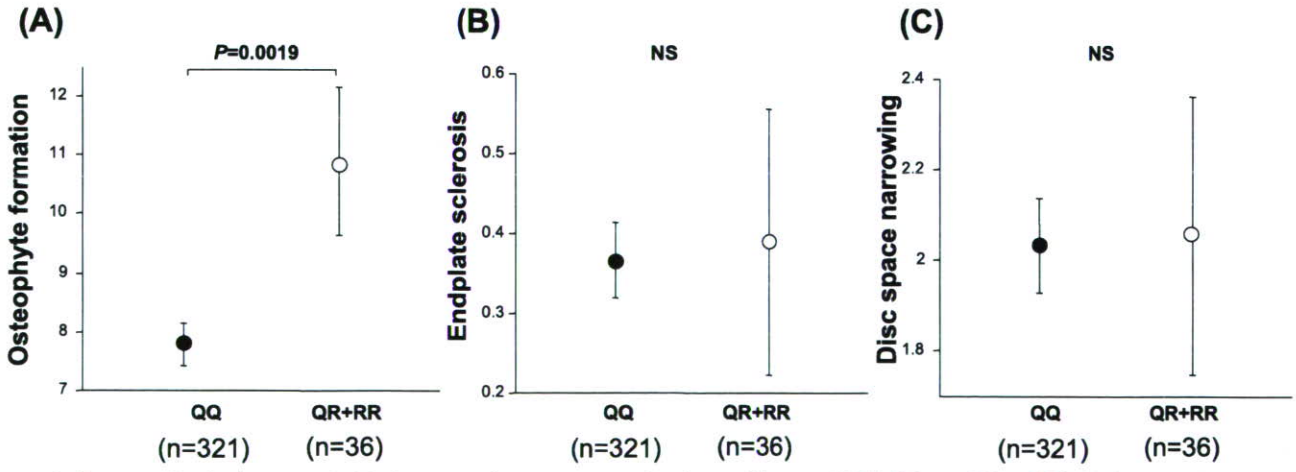

Figure 1. Scores of spinal osteoarthritis between the genotypes of polymorphism at Q89R (QQ *vs.* QR + RR). **A**, Scores of osteophyte formation are shown for genotype QQ and for genotype QR + RR. Scores are expressed as mean ± SE. Numbers of subjects are shown in parentheses. **B**, Scores of endplate sclerosis. **C**, Disc space narrowing scores. The association of the two genotype groups with osteoarthritis parameters was determined by ANCOVA, a type of multifactorial analysis, with adjustment of confounding clinical variables (age, body weight, and height).

other joints. It is also reported that there was a significant association of a functional gene variant of secreted frizzled-related protein 3 (sFRP3), which antagonizes Wnt signaling, with hip osteoarthritis in women.[31] Taken together, our results and the recent evidence suggest that the canonical Wnt signaling pathway including LRP5 is critical in the pathogenesis of skeletal abnormality, including osteoarthritis and osteoporosis.

Recently, mutations of the LRP5 gene have been described to be associated with both osteoporosis-pseudoglioma syndrome and the high bone mass phenotype.[18–21] It was found that loss-of-function of LRP5 in both human[18] and mice[19] yielded a decrease in bone formation, or an active mutation of LRP5 that cannot bind to a Wnt inhibitor Dickkopf-1 resulted in a high bone mass trait.[20,21] Moreover, our group and several other groups have reported that single-nucleotide polymorphisms in LRP5 gene predicted the bone mass.[27,32–36] These SNPs included three of different missense variations; Q89R,[33,34] V667 M,[35] and A1330V.[36] In the present study, we investigated a possible contribution of Q89R LRP5 polymorphism to spinal osteoarthritis in Japanese women. V667 M polymorphism was not detected in our Japanese population. Regarding A1330V polymorphism, we could not detect an association of the SNP with spinal osteoarthritis (data not shown).

Two groups reported consistent association of Q89R with Ward's triangle BMD but not with lumbar BMD in Korean young men[33] and Chinese premenopausal women.[34] In our Japanese population, we did not find an association of Q89R polymorphism with lumbar spine. The present data together with published data related to osteoporosis suggest that Q89R polymorphism may be involved in the pathogenesis of both osteoporosis and spinal osteoarthritis and QQ genotype in LRP5 might be preventive for both diseases. Meanwhile, there are other cases in which genetic factors contribute to the pathogenesis of osteoporosis and osteoarthritis in an opposite way. For example, it has been reported that transforming growth factor-β1 (TGF-β1) gene polymorphism T869C, which gives Leu>Pro substitution contributes differentially to osteoporosis and osteoarthritis; people with CC genotype had significantly higher BMD than those with TC or TT, whereas this CC genotype was related to significantly greater osteophytes than TT or TC.[37]

Osteoarthritis occurs as result of both mechanical and biologic events that destabilize the normal coupling of degradation and synthesis of articular cartilage chondrocytes and extracellular matrix as well as subchondral bone.[1,38] Cartilage destruction during osteoarthritis involves the loss of differentiated phenotype and apoptotic death of chondrocytes,[39] Wnt proteins were shown to regulate dedifferentiation of apoptosis of chondrocytes.[40] It is also demonstrated the interaction of β-catenin with SOX9, a transcriptional factor that is required in successive steps of chondrogenesis, controls chondrocyte differentiation.[41] These data suggest Wnt/β-catenin may participate in the pathogenesis of cartilage diseases, such as osteoarthritis. Further studies will be required to clarify the role of Q89R missense variant of the LRP5 in the pathogenesis of osteophyte formation and osteoporosis.

■ Conclusion

We have shown an association of the Q89R polymorphism in the LRP5 gene with a radiographic feature of spinal osteophytosis in postmenopausal Japanese women. The women with QQ genotypes had significantly lower osteophyte formation scores. The LRP5 genotyping might be beneficial in the prevention and management of spinal osteophytosis as well as osteoporosis. The present findings regarding the correlation of LRP5 polymorphism with spinal osteoarthritis provide a new promising direction for the clinical medicine of the spine disease, which leads us to the development of new diagnostic markers as well as therapeutic options based on the molecular target.

■ Key Points

- Wnt/β-catenin signaling pathway regulates bone and cartilage metabolism.
- The single-nucleotide polymorphism, causing an amino-acid change (Q89R) in LRP5 gene that encodes a Wnt coreceptor, was associated with spinal osteophytosis in Japanese postmenopausal women.
- We suggest that a genetic variation at the LRP5 gene locus is associated with spinal osteoarthritis.

References

1. Creamer P, Hochberg MC. Osteoarthritis. *Lancet* 1997;350:503–8.
2. Lane NE, Nevitt MC, Hochberg MC, et al. Reliability of new indices of radiographic osteoarthritis of the hand and hip and lumbar disc degeneration. *J Rheumatol* 1993;20:1911–8.
3. O'Neill TW, McCloskey EV, Silman AJ, et al. The distribution, determinants, and clinical correlates of vertebral osteophytosis: a population based survey. *J Rheumatol* 1999;26:842–8.
4. Spector TD, MacGregor AJ. Risk factors for osteoarthritis: genetics. *Osteoarthritis Cartilage* 2004;12(suppl):39–44.
5. Loughlin J. Genetics of osteoarthritis and potential for drug development. *Curr Opin Pharmacol* 2003;3:295–9.
6. Nusse R, Varmus HE. Wnt genes. *Cell* 1992;69:1073–87.
7. Rijsewijk F, Schuermann M, Wagenaar E, et al. The Drosophila homolog of the mouse mammary oncogene int-1 is identical to the segment polarity gene wingless. *Cell* 1987;50:649–57.
8. Nusse R, Varmus HE. Many tumors induced by the mouse mammary tumor virus contain a provirus integrated in the same region of the host genome. *Cell* 1982;31:99–109.
9. Barrow JR, Thomas KR, Boussadia-Zahui O, et al. Ectodermal Wnt3/beta-catenin signaling is required for the establishment and maintenance of the apical ectodermal ridge. *Genes Dev* 2003;17:394–409.
10. Soshnikova N, Zechner D, Huelsken J, et al. Genetic interaction between Wnt/beta-catenin and BMP receptor signaling during formation of the AER and the dorsal-ventral axis in the limb. *Genes Dev* 2003;17:1963–8.
11. Cadigan KM, Nusse R. Wnt signaling: a common theme in animal development. *Genes Dev* 1999;11:3286–305.
12. Derfoul A, Carlberg AL, Tuan RS, et al. Differential regulation of osteogenic marker gene expression by Wnt-3a in embryonic mesenchymal multipotential progenitor cells. *Differentiation* 2004;72:209–23.

13. Bennett CN, Longo KA, Wright WS, et al. Regulation of osteoblastogenesis and bone mass by Wnt10b. *Proc Natl Acad Sci USA* 2005;102:3324–9.
14. Bain G, Muller T, Papkoff J, et al. Activated beta-catenin induces osteoblast differentiation of C3H10T1/2 cells and participates in BMP2 mediated signal transduction. *Biochem Biophys Res Commun* 2003;301:84–91.
15. Zhou S, Eid K, Glowacki J. Cooperation between TFG-beta and Wnt pathways during chondrocyte and adipocyte differentiation of human marrow stromal cells. *J Bone Miner Res* 2004;19:463–70.
16. Tamai K, Semenov M, Kato Y, et al. LDL-receptor-related proteins in Wnt signal transduction. *Nature* 2000;407:530–5.
17. Mao J, Wang J, Liu B, et al. Low-density lipoprotein receptor-related protein-5 binds to Axin and regulates the canonical Wnt signaling pathway. *Mol Cell* 2001;7:801–9.
18. Gong Y, Slee RB, Fukai N, et al. LDL receptor-related protein 5 (LRP5) affects bone accrual and eye development. *Cell* 2001;107:513–23.
19. Kato M, Patel MS, Levasseur R, et al. Cbfa1-independent decrease in osteoblast proliferation, osteopenia, and persistent embryonic eye vascularization in mice deficient in Lrp5, a Wnt coreceptor. *J Cell Biol* 2002;157:303–14.
20. Boyden LM, Mao J, Belsky J, et al. High bone density due to a mutation in LDL-receptor-related protein 5. *N Engl J Med* 2002;346:1513–21.
21. Little RD, Carulli JP, Del Mastro RG, et al. A mutation in the LDL receptor-related protein 5 gene results in the autosomal dominant high-bone-mass trait. *Am J Hum Genet* 2002;70:11–9.
22. Sen M, Lauterbach K, Carson DA, et al. Expression and function of wingless and frizzled homologs in rheumatoid arthritis. *Proc Natl Acad Sci USA* 2000;97:2791–6.
23. James IE, Kumar S, Lark MW, et al. FrzB-2: a human secreted frizzled-related protein with a potential role in chondrocyte apoptosis. *Osteoarthritis Cartilage* 2000;8:452–63.
24. Ryu JH, Kim SJ, Chun JS, et al. Regulation of the chondrocyte phenotype by beta-catenin. *Development* 2002;129:5541–50.
25. Yu W, Gluer CC, Fuerst T, et al. Influence of degenerative joint disease on spinal bone mineral measurements in postmenopausal women. *Calcif Tissue Int* 1995;57:169–74.
26. Asai T, Ohkubo T, Katsuya T, et al. Endothelin-1 gene variant associates with blood pressure in obese Japanese subjects: the Ohasama Study. *Hypertension* 2001;38:1321–4.
27. Urano T, Shiraki M, Inoue S, et al. Association of a single-nucleotide polymorphism in low-density lipoprotein receptor-related protein 5 gene with bone mineral density. *J Bone Miner Metab* 2004;22:341–5.
28. Chapman K, Mustafa Z, Loughlin J, et al. Osteoarthritis-susceptibility locus on chromosome 11q, detected by linkage. *Am J Hum Genet* 1999;65:167–74.
29. Chapman K, Mustafa Z, Loughlin J, et al. Finer linkage mapping of primary hip osteoarthritis susceptibility on chromosome 11q in a cohort of affected female sibling pairs. *Arthritis Rheum* 2002;46:1780–3.
30. Smith AJ, Gidley J, Mansell JP, et al. Haplotypes of the low-density lipoprotein receptor-related protein 5 (LRP5) gene: are they a risk factor in osteoarthritis? *Osteoarthritis Cartilage* 2005;13:608–13.
31. Loughlin J, Dowling B, Corr M, et al. Functional variants within the secreted frizzled-related protein 3 gene are associated with hip osteoarthritis in females. *Proc Natl Acad Sci USA* 2004;101:9757–62.
32. Koay MA, Brown MA. Genetic disorders of the LRP5-Wnt signalling pathway affecting the skeleton. *Trends Mol Med* 2005;11:129–37.
33. Koh JM, Jung MH, Kim GS, et al. Association between bone mineral density and LDL receptor-related protein 5 gene polymorphisms in young Korean men. *J Korean Med Sci* 2004;19:407–12.
34. Lau HH, Ng MY, Kung AW, et al. Genetic and environmental determinants of bone mineral density in Chinese women. *Bone* 2005;36:700–9.
35. Ferrari SL, Deutsch S, Antonarakis SE, et al. Polymorphisms in the low-density lipoprotein receptor-related protein 5 (LRP5) gene are associated with variation in vertebral bone mass, vertebral bone size, and stature in whites. *Am J Hum Genet* 2004;74:866–75.
36. Mizuguchi T, Furuta I, Yoshiura K, et al. LRP5, low-density-lipoprotein-receptor-related protein 5, is a determinant for bone mineral density. *J Hum Genet* 2004;49:80–6.
37. Yamada Y, Okuizumi H, Harada A, et al. Association of transforming growth factor beta1 genotype with spinal osteophytosis in Japanese women. *Arthritis Rheum* 2000;43:452–60.
38. Hamerman D. Aging and osteoarthritis: basic mechanisms. *J Am Geriatr Soc* 1993;41:760–70.
39. Sandell LJ, Aigner T. Articular cartilage and changes in arthritis: an introduction: cell biology of osteoarthritis. *Arthritis Res* 2001;3:107–13.
40. Hwang SG, Ryu JH, Chun JS, et al. Wnt-7a causes loss of differentiated phenotype and inhibits apoptosis of articular chondrocytes via different mechanisms. *J Biol Chem* 2004;279:26597–604.
41. Akiyama H, Lyons JP, de Crombrugghe B, et al. Interactions between Sox9 and beta-catenin control chondrocyte differentiation. *Genes Dev* 2004;18:1072–87.

J Bone Miner Metab (2007) 25:253–258
DOI 10.1007/s00774-007-0757-9

ORIGINAL ARTICLE

**Tomohiko Urano · Ken'ichiro Narusawa
Masataka Shiraki · Takahiko Usui · Noriko Sasaki
Takayuki Hosoi · Yasuyoshi Ouchi · Toshitaka Nakamura
Satoshi Inoue**

Association of a single nucleotide polymorphism in the WISP1 gene with spinal osteoarthritis in postmenopausal Japanese women

Received: December 19, 2006 / Accepted: January 31, 2007

Abstract The Wnt-β-catenin signaling pathway that regulates bone density is also involved in cartilage development and homeostasis in vivo. Here, we assumed that genetic variation in Wnt-β-catenin signaling genes can affect the pathogenesis of cartilage related diseases, such as osteoarthritis. Wnt-1-induced secreted protein 1 (WISP1) is a target of the Wnt pathway and directly regulated by β-catenin. In the present study, we analyzed the association of a single nucleotide polymorphism (SNP) in the WISP1 3′-UTR region with the development of radiographically observable osteoarthritis of the spine. For this purpose, we evaluated the presence of osteophytes, endplate sclerosis, and narrowing of disc spaces in 304 postmenopausal Japanese women. We compared those who carried the G allele (GG or GA, $n = 184$) with those who did not (AA, $n = 120$). We found that the subjects without the G allele (AA) were significantly over-represented in the subjects having higher endplate sclerosis score ($P = 0.0069$; odds ratio, 2.91; 95% confidence interval, 1.34–6.30 by logistic regression analysis). On the other hand, the occurrence of disc narrowing and osteophyte formation did not significantly differ between those with and without at least one G allele. Thus, we suggest that a genetic variation in the WISP1 gene locus is associated with spinal osteoarthritis, in line with the involvement of the Wnt-β-catenin-regulated gene in bone and cartilage metabolism.

Key words single nucleotide polymorphism (SNP) · Wnt-β-catenin signaling · WISP1 · osteoarthritis · endplate sclerosis

T. Urano · T. Usui · N. Sasaki · Y. Ouchi · S. Inoue (✉)
Department of Geriatric Medicine, Graduate School of Medicine, The University of Tokyo, 7-3-1 Hongo, Bunkyo-ku, Tokyo, 113-8655 Japan
e-mail: INOUE-GER@h.u-tokyo.ac.jp
Tel. +81-3-5800-8652; Fax +81-3-5800-6530

T. Urano · S. Inoue
Department of Coca-Cola Anti-Aging Medicine, Graduate School of Medicine, The University of Tokyo, Tokyo, Japan

K. Narusawa · T. Nakamura
Department of Orthopedic Surgery, University of Occupational and Environmental Health, School of Medicine, Kitakyushu, Japan

M. Shiraki
Research Institute and Practice for Involutional Diseases, Nagano, Japan

T. Hosoi
Department of Advanced Medicine, National Center for Geriatrics and Gerontology, Aichi, Japan

S. Inoue
Research Center for Genomic Medicine, Saitama Medical School, Saitama, Japan

Introduction

Spinal osteoarthritis is a highly prevalent musculoskeletal disorder and a major cause of back symptoms [1]. Vertebral osteophytes, endplate sclerosis, and intervertebral disc narrowing are recognized as characteristic features of spinal degeneration. Recent studies indicate that the appearance of these radiographic features is influenced by physical loading and other environmental factors [2,3]. Moreover, spinal osteoarthritis has been shown to have a familial component and in some studies to be influenced by specific genetic risk factors, mainly by investigating genes encoding structural proteins of the extracellular matrix of cartilage (e.g., collagen type II α1, cartilage matrix protein, and aminoguanidine) or genes playing a role in the regulation of bone density and mass (e.g., vitamin D receptor, insulin-like growth factor-I, and estrogen receptor-α) [4,5].

The Wnt (wingless-type MMTV integration site family) represents a large group of secreted signaling proteins that are involved in cell proliferation, differentiation, and morphogenesis [6]. The name 'Wnt' is derived from *wingless* gene in *Drosophila melanogaster* [7] and murine *int-1* oncogene identified in tumors induced by mouse mammary tumor virus [8]. It is also known that Wnt and bone morphogenetic protein (BMP) signals control apical ectodermal ridge (AER) formation and dorsoventral patterning during limb development [9,10]. Wnt proteins activate signal transduction through Frizzled, which act as receptors for

Wnt proteins [11] and induce stabilization of cytoplasmic β-catenin protein, which also regulates target gene expression as a transcriptional coactivator. The physiological role of the Wnt in the regulation of osteoblastogenesis has been studied in experimental models. Mice expressing Wnt10b transgene in bone marrow have shown high bone mass by simulating osteoblastogenesis [12]. It is also shown that activated β-catenin stimulates osteoblast differentiation [13]. Further, low-density lipoprotein (LDL)-receptor-related protein 5 and 6 (LRP5/6) were also found to be required for Wnt coreceptors [14,15]. Recent reports demonstrated that the Wnt/β-catenin signaling pathway regulates bone mineral density (BMD) through LRP5 [16–19]. Moreover, we and several groups reported that single nucleotide polymorphisms (SNPs) in the LRP5 gene predicted bone mass [20–23]. These findings indicate that the Wnt-β-catenin signaling pathway plays important roles in skeletal biology.

In addition to the regulation of limb development and bone metabolism, Wnt/β-catenin signaling may be involved in the maintenance and pathophysiology of cartilage. This possibility is indirectly supported by the observation that several Wnt proteins and Frizzled receptors are expressed in the synovial tissue of arthritic cartilage [24]. In addition, a secreted Frizzled-related protein (FrzB-2) that act as an antagonist for Frizzled receptor is strongly expressed in osteoarthritic cartilage and may regulate chondrocyte apoptosis [25]. It is also shown that chondrocytes express β-catenin at a low level and that an accumulation of β-catenin is sufficient to cause dedifferentiation of chondrocytes, suggesting that Wnt signaling is involved in cartilage metabolism [26].

Wnt-1-induced secreted protein 1 (WISP1) is a member of the CCN family growth factors, which includes connective tissue growth factor (CTGF), cysteine-rich 61 (Cyr61), nephroblastoma overexpressed (NOV), WISP2, and WISP3 [27–30]. WISP1 is a target of the Wnt/β-catenin pathway, and its expression is regulated by β-catenin [30,31]. WISP1 activity and availability are modulated by its interaction with decorin and biglycan, two extracellular matrix-associated proteoglycans found abundantly in bone and cartilage [32]. In mouse chondrocytic cell lines, WISP1 increased proliferation and saturation density but repressed chondrocytic representation [33]. These data suggest that WISP1 could play an important regulatory role in bone and cartilage homeostasis. In the present study, we examined an association between a polymorphism in the WISP1 gene and radiographic features of spinal osteoarthritis including osteophyte formation, endplate sclerosis, and disc space narrowing to investigate a possible contribution of WISP1 to human bone and cartilage metabolism.

Materials and methods

Subjects

Genotypes were analyzed in DNA samples obtained from 304 healthy postmenopausal Japanese women (mean age ± SD, 66.3 ± 9.0) living in the central area of Japan. Exclusion criteria included endocrine disorders such as hyperthyroidism, hyperparathyroidism, diabetes mellitus, liver disease, renal disease, use of medications known to affect the bone metabolism (e.g., corticosteroids, anticonvulsants, heparin sodium), or unusual gynecological history. Patients with severe hip and knee arthritis were excluded from the present study. The eligibility of subjects was determined by taking the history and physical examination. All were nonrelated volunteers and provided informed consent before this study. Ethical approval for the study was obtained from appropriate ethics committees.

Radiographic grading of spinal osteoarthritis

Conventional thoracic and lumbar spinal plain roentgenograms in lateral and anteroposterior projection were obtained from all participants. The severities of spinal degeneration including osteophyte formation, endplate sclerosis, and disc space narrowing were assessed semiquantitatively from T4–T5 to L4–L5 disc level or from T4 to L5 vertebrae by using the grading scale of Genant [34]. Briefly, osteophyte formation at a given disc was graded 0–3 degrees, endplate sclerosis at given vertebra was graded 0–2 degrees, and disc space narrowing was graded 0–1 degrees. Then, we defined the sum of each degree from T4–T5 to L4–L5 disc level for osteophyte formation on anteroposterior radiographs as a score of osteophyte formation. We also defined the sum of each degree from T4 to L4 vertebra for endplate sclerosis and that from T4–T5 to L4–L5 disc level for disc space narrowing on lateral radiographs as a score of endplate sclerosis and disc narrowing, respectively. These semiquantitaive gradings on radiographics were performed by two expert medical doctors.

Determination of a SNP in the WISP1 gene

We extracted a polymorphic variation in the WISP1 gene exon 5 3′-untrans lated region (UTR) from the Assays-on-Demand SNP Genotyping Products database (Applied Biosystems, Foster City, CA, USA) and, according to its localization on the gene, denoted it 2364A/G. We determined the 2364A/G polymorphism of the WISP1 gene using the TaqMan (Applied Biosystems) polymerase chain reaction (PCR) method [35]. To determine the WISP1 SNP, we used Assays-on-Demand SNP, Genotyping Products C_9086661_10 (Applied BioSystems) (rs2929970), which contains sequence-specific forward and reverse primers and two TaqMan MGB probes for detecting alleles. During the PCR cycle, two TaqMan probes competitively hybridize to a specific sequence of the target DNA and the reporter dye is separated from the quencher dye, resulting in an increase in fluorescence of the reporter dye. The fluorescence levels of the PCR products were measured with the ABI PRISM 7000, resulting in clear identification of three genotypes of the SNP.